



UNIVERSIDAD DE GUANAJUATO

CAMPUS Irapuato-Salamanca

DIVISIÓN DE INGENIERÍAS

**DESIGN OF STRUCTURAL PROFILES WITH
INTERLAMINAR REINFORCEMENTS IN COMPOSITES**

A thesis for the degree of:

Master in science (M.Sc.) in

Mechanical Engineering

OMAR CAMILO HORTÚA DÍAZ

ADVISOR:

DR. VICTOR ALFONSO RAMÍREZ ELÍAS

SALAMANCA, GTO.

OCTOBER 2019

CONTENTS

Abstract.....	7
Publications	8
Acknowledgments	9
1 <i>Introduction</i>	10
1.1 Objectives.....	10
1.2 Background	11
1.3 Contribution	12
2 <i>Literature review</i>	13
2.1 Introduction.....	13
2.2 Major applications.....	13
2.3 Most relevant applications	14
2.4 Configuration and fibre variations	15
2.5 Composites beams.....	16
2.6 Composites beams with interlaminar reinforcements	19
2.7 Beams and joints	20
2.7.1 I-beams	20
2.7.2 T-beams	22
2.7.3 T-joints	23
2.8 Interlaminar reinforcement: Nonwoven veils	25
2.9 Final remark	26
3 <i>Experiment method and materials</i>.....	28
3.1 Introduction.....	28
3.2 Materials.....	28

3.2.1	Matrix	28
3.2.2	Reinforcements	29
3.2.3	Interlaminar veils	30
3.3	Fixture	31
3.3.1	First design of test rig.....	32
3.3.2	Second design of test rig	33
3.3.3	Third design for test rig	35
3.3.4	Design of test support base	36
3.4	Especimens characteristics	38
3.5	Curing and veil characterisation.....	39
3.5.1	Characterisation of curing time resin	39
3.5.2	Resin characterisation under tensile tests	39
3.5.3	Characterisation of veil tensile strength in out-of-plane direction	41
3.6	Veils incorporation	42
3.6.1	Fabric	43
3.6.2	Incorporation process	43
3.7	Mechanic characterisation	44
3.8	Final remarks.....	46
4	Static tests.....	47
4.1	Introduction.....	47
4.2	Behaviour of base specimens.....	47
4.3	Reinforced specimens with PPS veils.....	50
4.4	Discussion	51
5	Modeling by finite element method	54
5.1	Introduction.....	54
5.2	Modeling of I and T beams	54
5.2.1	Geometrical modeling	55
5.2.2	Materials.....	56
5.2.3	Elementes	57
5.2.4	Mesh	59
5.2.5	Boundary conditions	61

5.2.6	Load	61
5.2.7	Postprocessor	62
6	<i>Conclusions and future work</i>	64
6.1	Conclusions.....	64
6.2	Future work	65
A.	<i>Manufacturer catalog for I and T-beams</i>	66
B.	<i>Published paper in congress</i>	67
C.	<i>Published poster</i>	74

FIGURES

FIGURE 2.1: A FAILURE OCCURRED IN ONE COMPOSITES TURBINE [19].....	15
FIGURE 2.2: PULTRUSION PROCESS [33].....	16
FIGURE 2.3: VARTM PROCESS FOR LAMINATED COMPOSITES [34]	17
FIGURE 3.1: INTERLAMINAR VEIL.....	31
FIGURA 3.2: ESQUEMA DE PRUEBA DE TRES PUNTOS.....	32
FIGURA 3.3: FIRST DESIGN FOR TEST RIG IN POSITION FOR) I-BEAMS AND B) T-BEAMS.	33
FIGURE 3.4: SECOND DESIGN FOR TEST RIG IN POSITION FOR A) I-BEAMS AND B) T-BEAMS....	35
FIGURA 3.5: THIRD DESIGN OF TEST RIG; A) CAD MODEL, B) MANUFACTURED PRODUCT.	36
FIGURE 3.6: DEVICE SUPPORT FOR SPECIMENS.....	37
FIGURA 3.7: FINAL PRODUCT OF TEST RIG.....	37
FIGURA 3.8: ESPECÍMENES BASE CON GEOMETRÍA I Y T.....	38
FIGURE 3.9: SAMPLE TO PERFORM TENSILE TEST	40
FIGURE 3.10: DATA FROM TENSILE TESTS FOR RESIN SYSTEM.....	40
FIGURE 3.11: SPECIMENS BEFORE AND AFTER THE TEST	42
FIGURE 3.12: TENSILE TEST FOR PPS VEILS IN OUT-OF-PLANE DIRECTION.....	42
FIGURA 3.13: VEIL INCORPORATION PROCESS; A) RESIN PREPARATION, VEILS AND CARBON FIBRE FABRICS B) VEIL PLACEMENT, C) FIBRE CARBON PLACEMENT, D) SPECIMENS AFTER CURING PROCESS.	44
FIGURE 4.1: REINFORCED AND BASE SPECIMENS.....	47
FIGURE 4.2: RESULTS OF BASE SPECIMENS; A) I GEOMETRY, B) T GEOMETRY.	49
FIGURA 4.3: RESULTS OF REINFORCED BEAMS; A) I GEOMETRY, B) T GEOMETRY.....	51
FIGURE 4.4: TEST IN I-BEAMS WITHOUT BENDING, A) BASE SPECIMEN B) REINFORCED SPECIMEN ...	53
FIGURA 4.5: COMPARISON BETWEEN BASE AND REINFORCED; A) I-BEAMS, B) T-BEAMS.....	54
FIGURE 5.1 LINES IN GEOMETRICAL MODELS DE LAS VIGAS I Y T.	55
FIGURE 5.2: AREA IN GEOMETRICAL MODELS FOR FEA IN I AND T BEAMS.....	56
FIGURE 5.3: ELEMENT DESCRIPTION "SHELL 181".	57
FIGURE 5.4 ELEMENT DESCRIPTION "SOLID 185".	59
FIGURE 5.5: GENERAL MESH OF MODELS	60
FIGURE 5.6: STACKING SEQUENCE AS BEAMS THICKNESS; A) T-BEAM, B) I-BEAM, C) EPOXY RESIN VOLUME.	61
FIGURE 5.7: TSAI-WU INDICES FOR THE WHOLE MODEL AND THE REGION MADE BY RESIN; A) I- BEAM, B) T-BEAM.	63

TABLES

TABLE 3.1: RESIN AND HARDENER SPECIFICATIONS.....	29
TABLE 3.2: PROCESSING DATA FOR EPOXY RESIN SYSTEM.....	30
TABLA 3.3: FABRICS ORIENTATION	30
TABLE 4.1: RESULTS OF I-BEAM BASE SAMPLE.....	48
TABLA 4.2: RESULTS OF T-BEAM BASE SAMPLE.....	48
TABLE 4.3: RESULTS OF I-BEAMS FOR FLEXURAL TEST.	50
TABLE 4.4: RESULTS OF T-BEAMS FOR FLEXURAL TEST.	50
TABLA 5.1 MATERIAL FOR FEA MODEL OF BEAMS	57
TABLE 5.2: STRESSES AND TSAI-WU INDEX FOR BEAMS.	62

ABSTRACT

Universidad de Guanajuato

Omar Camilo Hortúa Díaz

Design of structural profiles with interlaminar reinforcement in composites

2019

Ultralight-weight structures are an application of composites attracting industries attention, especially, aircraft and energy ones. In the latter, as transport and wind energy in the blades and support fabrication. The weight-stresses relation is one of the great ambitions to improve, however, the solution cannot be only a base composite material because of the weak present areas where there is no fibre reinforcement and thus it would expect the initiation crack. Therefore, the main of this study is established, which focuses on the modification and improvement of basic structures I and T, in order to decrease structures weight or increase mechanical properties, particularly, flexural strength. To achieve this goal, an I-beam manufactured was acquired, manufactured using the vacuum-assisted resin-molded technique composed by carbon fibre and epoxy resin. The structures have been modified with PPS veil introduction which is an interlaminar reinforcement offering an increase in fracture resistance, and therefore, delay the crack propagation. Concerning to I and T-beams tests, there are no standardized dimensions and no geometries; as well as no fixture design or test procedures. In the early stages, the test equipment had to be designed and set procedure parameters for performing a quasi-static process. A FE analysis was carried out to detect critical points on each beam, highlighting those on the central plane where one of the rollers was making contact, showing a Tsai-Wu index close to 1 for both configurations, announcing the point where the failure will occur which is part of a region where there no fibre reinforcement. Test results were compared, and it was obtained a fourfold improvement among veil reinforced beams respect to the base specimens.

LIST OF PUBLICATIONS

- Congress:
 - Hortúa Díaz Omar Camilo, Ramírez Elías Víctor Alfonso; “A review of the experimental progress of composites beams as lightweight structures and their in and out-of-plane properties”; XXV Congreso internacional anual de la SOMIM; 18-20 September 2019, Mazatlán, Mexico.
- Poster presentation:
 - Hortúa-Díaz O.C., Ramírez-Elías V.A.; “Design of structural profiles with interlaminar reinforcement in composites”; Mechanical Engineering week Dr. Ricardo Chicuriel Uziel; Universidad de Guanajuato; 25-29 March 2019, Salamanca, México.

ACKNOWLEDGMENTS

I affectionately dedicate this thesis to my parents and sister who always give me moral support and inspiration throughout my life, motivating me to constantly climb steps. To my girlfriend Cielo, for her unconditional support.

Infinite gratitude to my supervisor Dr. Víctor Alfonso Ramírez Elías, for his excellent and successful guide, in addition to the effort shown through the development of this work, helping me with his academic, professional and personal advices, a utopia that rarely comes true.

I extend my thanks to the National Council of Science and Technology – CONACYT which has funded my scholarship during my master course duration. To the University of Guanajuato, for the support granted for the research visit and presentation carried out. Finally, I would like to thank my friends of my academic generation: Juan, Mauricio, Tomás, Esteban and Carlos for their understanding and help in times of difficulty. Their friendship together with my tutor's guidance made my master's course an enriching experience in several aspects.

INTRODUCTION

This thesis work reports an investigation carried out in the División de ingenierías, Universidad de Guanajuato between 2017 and 2019. The purpose of this project was to investigate the effect of an interlaminar reinforcement on structural profiles of laminated composite material for the use of ultralight structures. Some of the specific objectives of this research are:

1. To examine the influence of the longitudinal insertion of veils through the middle plane on the flexural strength of a structural element, I and T beams, of laminated composite material.
2. To detect and explain the critical points of failure using an analysis of finite elements involved in the flexural tests.
3. To compare the results obtained experimentally with the data obtained from FEA.

1.1 Objectives

General objective

Design and characterization of structural profiles of laminated composite materials with an improvement in their flexural resistance through the selection of interlaminar reinforcements for the use of ultralight-weight structures.

Specific objectives

- Versatile test equipment design for two cross sections I and T.
- Development of a test protocol for flexural tests in structural profiles.

- Performance of flexural tests of 3 contact points under static load in both geometries.
- Analysis of the results of the base specimens with respect to the reinforced ones.

1.2 Background

Regarding general objective development, some methods used to improve the toughness to the interlaminar fracture were extensively studied. Some of these methods are the addition of fibers by means of layers of non-woven veils, tufting, stitching, z-pinning and others to add a reinforcement through the thickness and delay the delamination or debonding between matrix and fibers at large loads.

The performance improvement of composite materials through thickness management has been a topic of interest over the past 40 years. However, most of these studies have been practiced in materials composed of flat geometry evaluating properties distant to a structural behaviour under load. To work with a real part of a structural profile in this project, two basic structural sections, I and T beams were selected as structural representative parts. In addition, as there is no ASTM or ISO standard for an established method to perform flexural tests with this geometry and these materials; therefore, it was necessary to develop a test protocol as a complement to the available test equipment. Likewise, a finite element analysis was conducted using the Mechanical Ansys Parametric Design Language (APDL) software. As part of the work phase, the vertical speed of the load pusher was determined, fully defining the method that characterises I and T beams made of laminated composite materials.

Multiple techniques for the manufacture of laminated composites currently exist, among which are: autoclave, hand layup, prepeg moulding, resin transfer moulding (RTM), vacuum assisted resin transfer moulding (VARTM), each one has certain benefits and disadvantages. Respect to the manufacture of beams, pultrusion method is added to the previous techniques. The use of VARTM method in

manufacturing has increased significantly during the last three decades due to its low cost of production, repeatability, high finishes, the fusion of clean handling from RTM, flexibility and scalability as a result of hand layup method [1, 2]. However, since VARTM is a process in which the flow of resin through the thickness of the specimen prevails, interlaminar reinforcement techniques are limited. As an example, the methods that increase the viscosity of the resin would impede the total impregnation of the specimen, as well as others that consist of randomly positioning fibres that will be dragged and aligned with the direction of flow. Therefore, the veils belonging to the group of nonwoven fabrics become a viable reinforcement for VARTM and hand layup processes, highlighting their permeability and therefore allowing the resin to pass through the thickness.

Finally, after conducting the tests and based on the conclusions obtained in this project, future research work is suggested to further contribute to go further in this research area.

1.3 Contribution

The achievement of the objectives required the implementation of a flexural tests protocol for I and T beams made of laminated composite material, generating the design and manufacturing of a versatile equipment for both geometries, as well as the definition of dimensional parameters in specimen and displacement speed of the application load.

LITERATURE REVIEW

2.1 Introduction

In order to successfully address the problem of improving the mechanical properties in the basic structural sections made of composite materials typically used in the aerospace, bridge, wind and other energy industry, the acquisition of scientific knowledge through an extensive literary review was necessary. The study began by identifying the most commonly used manufacturing methods and interlaminar reinforcements with structural sections. Next, identifying the different geometries experienced as beams, their modifications to the composition and correspondingly alterations in the mechanical properties. When we talk about modifications, it is regarding methods to improve the interlaminar fracture toughness of these sections, among which are: carbon nanotubes (CNT), stitching and tufting. Although the pultrusion method is used with the same frequency as the vacuum assisted resin transfer moulding (VARTM) manufacturing technique in the industry, the latter stands out experimentally due to its operating cost.

2.2 Major applications

The ultralight basic structural sections arise from the need found in the 50s to find new materials that combine low weight and high toughness [3]. These two characteristics were the precursors to contemplate the use of composite materials, which are materials that have an excellent relation between specific stiffness and mechanical strength respect to weight. These structures are widely used throughout the industry, including automotive, thermal, aerial and optical [4–7], with the latter

focusing even more on dimensional stability, that is, a significant areal density regarding dimensions always sought in mirrors [8-9].

2.3 Most relevant applications

The energy industry, as same as the aforementioned applications, becomes important in the use of ultralight structures due to the greater ease achieved in the installation of electric power transport towers [10]. Although its application is not limited only to this kind of energy, it also stands out specifically in the wind energy industry, where these structures have a higher percentage of participation due to the constant optimization involved in their rapid expansion resulting from the generation of Clean energy [11, 12] and hindered only by the hearing pollution and air intermittency [11, 13].

Platts proposes an increase in the participation of composite materials in the wind energy industry, with respect to its current condition being only present in the blades of the turbines in the form of beams with cross-section I and T, the increase suggests a use in the bases of the highest towers found in offshore facilities, offering a decrease in corrosion and fatigue to which they are subjected [14]. Not all are advantages, there are also some adverse aspects such as the high cost of corrective maintenance due to sudden failures mostly present in the blades and which in turn is attributed 13.2% of failures of all turbines in Sweden [15], and which also represents one of the highest causes of failure in Germany [16], in other words, a ratio of 1 failure/turbine per year at least occurs throughout the wind farms (Figure 2.1) [17, 18].



Figure 2.1: A failure occurred in one composites turbine [19].

2.4 Configuration and fibre variations

There is a great variety of fibers and matrices in composite materials, yet with regard to ultralight structures, fibre reinforced thermoplastic materials are the most suitable and also bamboo strips stand out as natural fibres [20], however these fibres are rarely used. Apart from the characteristics mentioned in the previous section, there are also other benefits that are sought with these structures, which are mechanical strength, capacity for energy absorption, corrosion resistance and cost reduction in facilities [12], in particular, when these have a form of channel or I as the cross-section of structural elements [21, 22]. A successful example of the benefit achieved with the search for improvement of these properties has been a patent that reports a channel geometry which is capable of supporting 41,600 pounds with a thickness of 2 inches and distance between supports of 4 feet [22].

Although sandwich compounds are considered as ultralight structural materials, they are not widely used because their resistance in the out-of-plane direction is less than 10% of their equivalent in in-plane directions [23] and often fail when they are subjected to elastic buckling efforts [4, 24]. The most frequently used configuration is honeycomb, however, truss cores have more significant advantages due to their open structure [25]. On the other hand, a structure called biomimetics reinforced with tendons improves the properties in the outward direction of the plane by at least 2 times more than its equivalent in aluminium [24].

Another known configuration is the structure made of carbon-carbon composites, which become important when the volumetric expansion coefficient is an important design factor which is close to zero ($30 \times 10^{-6} \text{ K}^{-1}$) [3].

2.5 Composites beams

There are two methods with greater preponderance for the manufacture of composite materials, the pultrusion process being the most [26–31], consisting of the manipulation of fibres as fabric and being impregnated with resin and then passed through a mould to finish with a curing and cutting step (Figure 2.2)[32].

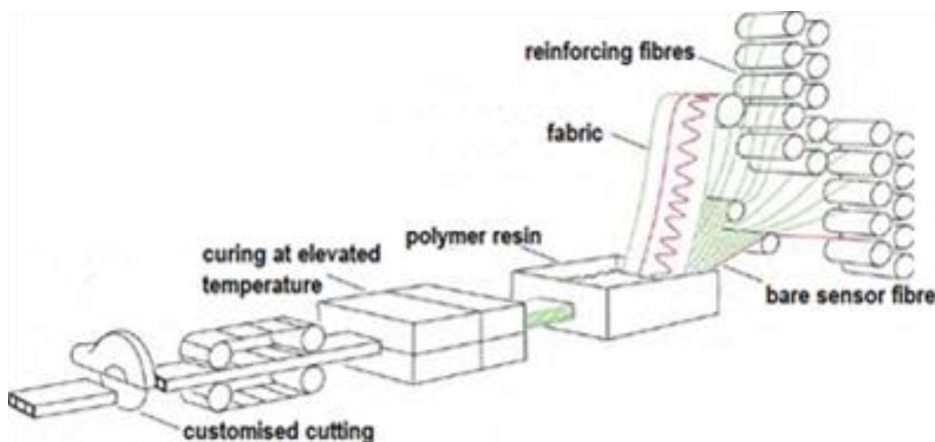


Figure 2.2: Pultrusion process [33].

Another technique frequently used for the manufacture of laminated beams is vacuum-assisted resin transfer molding VARTM (Figure 2.3).

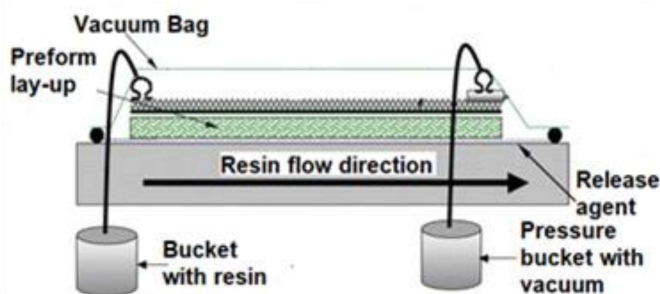


Figure 2.3: VARTM process for laminated composites [34].

In laminated composite materials, and thus in laminated beams, anisotropy stands out as the main characteristic, which means exceptional performance along the direction of the fibres, partially in disadvantage due to its deficient properties perpendicular to the fibres, triggering a significant possibility of a failure mode known as delamination caused mainly by interlaminar stresses [35].

Configurations in beams are crucial factors to avoid delamination, as a consequence, there were initially beams with a curved shape divided into two different geometries, elliptical and semicircular. The latter has two subtypes, one unscarfed, which reported 36.85 MPa of interlaminar tensile stress (ITS) under static load is only 63% of the in-plane transverse stress. While scarfed semi-circular specimens necked down at the test section with only 32.49 MPa of ITS, which represents 55% of the in-plane transverse stress. Finally, the elliptical samples had 107.06 MPa of TSI being 194% of the in-plane transverse stress. Moisture in the sample has a positive effect because it broadens the strength distribution; the mean ITS increased up to 107.9 MPa [35].

On the other hand, fatigue affects strength properties negatively, reducing the mean ITS to the middle at 10^6 cycles with no stable crack propagation [35]. When the failure occurs in flat and cylindrical composites beams, cracking in intraply matrix triggers delamination and begin the damage. Delamination can be stable and progressive if intraply bending cracks create this one; however, it can be the opposite if shear cracks induce it. Moreover, response and damage extension in composites are firmly related to ply orientation [36].

Hybrid composite beams are rare in industry application. Therefore, the studies focus on the improvements contributed by the FRP materials. As for wood, it can be bonded to FRP laminates, giving the raw material beam an increment when is two layered of up to 51% and 37% for CFRP and GFRP respectively, in flexural strength[37]. As reinforcements, non-uniformly graphene platelets (GPLs) were distributed in a polymer matrix which demonstrate a most effective way to reduce bending deflections, in addition, beams with a higher weight fraction of these reinforcements distributed symmetrically are less sensitive to the nonlinear

deformation [38]. Furthermore, the closer GPLs to the surface are the higher critical buckling load will suffer; this latter because GPL content affects positively also the postbuckling load-carrying[39].

Apart from the reinforcements, lamination scheme plays a vital role affecting critical buckling temperature, and thermal postbuckling path of the beam, where it can be concluded that stacking with excellent performance was $[0^\circ]_{10}$, where the subscript refers to the number of times that configuration repeats and has the highest critical buckling temperature. Moreover, the shear stiffness increment of the elastic foundation reduces the thermally induced postbuckling deflection of the beam [40]. On the other hand, reinforcements not only modify buckling phenomenon, but they also lead to a considerable improvement in beams, which is the case of a small portion of nanotubes [41].

Concerning optimisation through mathematical processes [42], Kalantari et al. [43] stated that exist matrix voids, fibre misalignment and thickness variation as primary obstacles to reaching a successful optimisation, similarly, Mejlej et al. [44] mentioned others such as fibre failure, matrix cracking and delamination initiation. Although almost every experimental research is made scaled-down, investigations pursue an aim which is applying to large-scale demanding time and economic resources, Asl et al. mentioned that scaled-down specimens behave similarly than those made in functional scale, focusing in remaining the aspect ratio [45–48].

At the same level of importance of optimisation, behaviour prediction under low-velocity impact can be found because of the internal damages induced by this speed, in consequence, Li et al. analysed its behaviour through an extended method where remarks that the delamination size, location on the maximum displacements and the matrix crack length influence on the performance beams [49].

2.6 Composites beams with interlaminar reinforcements

Composites beams suffer from the same disadvantages as composites, mainly, deficiency in out-of-plane mechanical properties. This latter justifies the insertion of

interlaminar reinforcements. Beams subjected to short beam shear testing with different material architecture showed there was a degradation in inter-laminar shear strength in those made of 3D woven compared to baseline plain woven composite. In contrast, there is an inversely proportional relationship between the fibers volume of z-yarns and the inter-laminar shear strength. In contrast, it can say 3D woven has more damage tolerance than 2D plain woven due to the distribution of damage in the post-elastic regime. Baseline materials have excellent properties in resistance to initial damage, but consecutively, this value decreases drastically as the energy increases [50].

When stitching as reinforcement is used in beams, stitch density profoundly influences the maximum load that a beam can support, modifying this property up to a 50% extra. Also, stitching and impact force does not correlate with beginning the delamination growth; however, after initiation, stitching parameters are essential for the extent of the delamination growth. This reinforcement is sufficient for high impact energy and delamination growth, and also when the delamination occurs in the middle of the thickness [51].

In concordance with Al-Khudairi et al. [52] y Ghasemnejad [53], stitched beams have a higher energy absorption capability and maintain the structural integrity for longer in composite wind turbine structure. Yarns volume is crucial in energy absorption because it allows the composite to support more energy impact but also increase displacement. In contrast with studies in [41–44], Ghasemnejad et al. [53] observed overlap region of joints stitched with Flax yarns increase the strength and impact energy absorption for nearly 70%.

Respect to interlaminar fracture toughness, Kim et. al. [54] shows that this property as opposed to the propagation and initiation energies which come from an impact, yet Ghasemnejad [53] contradicts the latter statement, showing among their results that interlaminar fracture toughness which was enhanced by flax stitching attracts the interlaminar crack propagation satisfactorily at the interface.

Another phenomenon which affects laminated beams is the buckling, and its sensitiveness depends significantly on the slenderness ratios (delamination length-

span length) [55]. Numerical approaches can also determine aspects for deformation, where it can be concluded that normal deformation effect depends on span-height ratio, boundary condition and lay-ups, in addition, for thick beams, clamped-clamped boundary conditions and unsymmetrical lay-up are more significant than others [56]. Similarly, Nguyen et al. work shows that the optimal solutions are linked to geometric parameters such as beam length, flanges width and web's height [57].

As another crucial characteristic of beams, stiffness varies in function of the flange height, increasing its value when T-beam flange height grows. Although this height has a positive effect on energy absorption which occurs due to bending of the beam, fibre breakage and matrix crack trigger, this feature is also related to the higher flexural stiffness and strength [58].

2.7 Beams and joints

2.7.1 I-beams

I and T shape classify as variations of the cross-sectional forms of beams. Composites can be utilized as the primary material for I-beams but also as a reinforcement of a metal I-beam as Lacki et al. stated [49, 50], where composites enhanced twice the buckling resistance and load-bearing capacity of an aluminium alloy I-beam when a mix of polyurethane foam and glass fibre in the flanges-web zone reinforced the structure. Although when it was combined with a CFRP on the flanges, the buckling resistance and load-bearing capacity increased four times respect to the plane aluminium I-beam [59].

When a composites beam is subjected to an environment with water, similarly with operational conditions of turbine blades, its interlaminar shear performance is reduced significantly. The reason is the cracks produced by fatigue cycling load in dry specimen were found on the inter-ply area while cracks in the immersed samples triggered the failure in the intraply area because of fibre/matrix debonding before the test [60].

An alternative method for pultruded I-beams consists in bonding web and flanges laminated with the resin being three different plates before realising and can be reinforced through a curb along the full length [61]. Feo et al. [61–63] studied the axial differences respect to a pultruded beams where mentioned axial stiffness were reduced dramatically from around 10 kN/mm to the middle in bonded beams (BB) and a quarter in reinforced bonded beam (RBB) when the specimen is subjected to an end-point load. However, when the load is placed in the middle the stiffness of pultruded beams, 11.32 kN/mm, is reduced to 80% for BB and the middle for RBB. In the other hand, these relationships are not present in the beam deformation because while BB is more brittle than the plane one and RBB presents a more ductile behaviour.

A combination of glass and carbon fibres restricted to flanges make a hybrid I-beam increasing structural performance, but only using glass fibres in the web minimising costs. Flange-web length ratio affects considerably to how failure occurs. In a rate of 0.43, beams behaviour was stable and linear under bending moment, while in the 1.13 ratio, the response was the opposite in the buckling and post-buckling region; however, both behavior configurations triggered failure delamination of the compressive flange [64]. Nevertheless, linear behaviour up to initial point failure in flexural, compression and tensile tests can be obtained by braiding, which also determines a performance without suffering delamination [65].

Other phenomena such as buckling and deflection which affect negatively I-beam are closely related to the increase in width and depth of unsupported flanges and web, as regards, the deflection is at its minimum value and critical buckling load at maximum value when the stacking sequences corresponds to $[0^\circ]_{2s}$ [66], where the subscript means a symmetric configuration and repeated twice.

Beams are affected significantly by the environment which they are exposed to, hence, Gagani et al. experimented with I-beams submerged into a fluid, contributing to a high rate of saturation in composites and concluding that fibre/matrix interface is a crucial aspect in the interlaminar shear fatigue performance and its immersed fatigue behaviour improved according to the resistance of the interface [60, 67].

2.7.2 T-beams

T-beams are also used as lightweight structures. A configuration to improve mechanical properties is manufacturing them through three-dimensional five-directional braided composites method at which there was a close correspondence between load-displacement curves (damage evolution) and stiffness degradation, showing a dependence of stiffness degradation with the stress level and the number of load cycles, decreasing the fatigue life with the incremental stress applied. Three stages of failure occurred in different parts, matrix cracks and resin-yarns interface debonding on the flange and fibre breaking in the web during the fatigue loading. Fibre breaking is the determinant factor for damage under the high-stress level; in contrast, the other two stages were prominent at low-stress level [68].

In some occasions, T-beams are subjected to high temperatures, where transverse impact behaviour becomes essential. Two factors influenced this behaviour, elevated temperature change failure mechanism from brittle to ductile while the temperature is increasing and transverse impact velocity being the most significant factor for transverse impact responses of the beam, which are impact peak load and total energy absorption [69]. While in a Biaxial Spacer Weft-Knitted Composite T-Beam, the impact loading is the most significant factor for the transverse impact responses [70]. Three failure mechanisms appeared in a 3D braided composites T-beam under transverse impact, matrix crack and fragmentation in the front surface and fibre breakage in the rear surface in the flange and the web position [69]. However, in a 3D orthogonal woven composite T-beam under same conditions, matrix crack occurred at the front surface, and in the meanwhile fibre breakage and matrix spallation appeared in the rear surface [71].

Yan et al. [72] compared the same reinforcement, 3D braiding, in T-beams and rectangular beams, noticing differences respect to the load-carrying capacity, where T-beams reported almost 20% of improvement respect to square ones. The increment of the number of cycles to failure under stress level of 80% was 789.6%,

while for 50% was 132%; thus, flexural rigidity is enhanced by the web reducing the tension loading region area of the lower surface in a fatigue test.

When it comes to the evaluation of web's height, the height as a parameter becomes crucial to energy absorption if compared to displacement, in other words, a height of 12 mm in the web contributes a growth in 15 J, which is a increment of 300%, of energy absorption when the displacement is 9 mm [73].

2.7.3 T-joints

T-joints are other cross-sectional composite structures which demand a significant interest of aircraft and wind energy industries. In many cases, their performance is closely related to bonding methods, surface preparation, adherend and geometrical properties [74–83], such parameters are important in the design and application of T-joints which have adhesion and bonding among their main feature [84]. However, these structures can be reinforced with through-thickness reinforcements such as z-pinning [68–84], stitching [75, 78–82, 85, 86] and tufting [87, 88].

Tan et. al. [89] found that Z-pinning technique does not modify the initial failure load due to the fillet region is not covered; thus this reinforcement only increased the ultimate strength in 18.3% respect to an adhered joint.

This feature and traction capacity can be supported because bridging traction formation triggered the crack. Thick skin affects positively showing a higher failure initiation strength in a limited deformation while thin skin may make bridging traction surpass the bending property of the skin. Z-pinning is also a sound reinforcement for out-of-plane tensile stress, increasing 13.6% the tensile strength for the adhesive connection mode and 0.83% about stitching method, and it complements with its high capacity to deform, being at least 20% more than the usual technique of adhesion [90].

However, within the in-plane directions, interlaminar reinforcements degrade the properties. 1-thread stitching process which was proposed to minimise the main

disadvantage of carbon threads, which is bending and thus preventing failure showed a reduction of around 17%, respect to unstitched specimens, but sharing values with z-pinning [91]. As a reinforced composite, it enhanced the pull-off failure strength in a range from 40.56% to 47.47% higher than the unreinforced ones, and even better than those with z-pinning reinforcement [91].

Damage detection in T-joints is indispensable to prevent crack propagation and avoid a total collapse in the structure. Li et al. [92, 93] proposed a mechanism to detect delamination in composite T-joints of wind turbines through the use of microwaves with an open-ended waveguide distinguishing the variation of flange thickness, the presence of the web incrusted into the flange and manufacturing defects. Detection could be focused primarily on the deltoid from the middle of the specimen where Xu et al. [94] noticed it is the more critical point for the beginning of Mode I debonding, on the other hand, the region with the highest stresses during mechanical pull-off load tests is at the free edges [95]. After detection, it is necessary to proceed with the repair, Cullinan et al. [96] tested to repair in situ with the use of embedded microvascular networks which create a way for the repair agent infiltration. Another method consists in creating a 3D healing network using stitching with mendable poly (ethylene-co-methacrylic acid) (EMAA) thermoplastic filament, and proceed with thermal activation which triggers repairs of delamination and matrix crack [97].

The out-of-plane mechanical properties are frequently insufficient for many applications. In response of that, Heimbs et al. [98] made tests with metallic arrow-pin reinforcement in a T-joint with multiples variations, where metal pins of maximum density and thermoplastic binder give an improvement in energy absorption of 720% respect to unreinforced T-joint in T-pull tests. Sandwich composite T-joints are also widely used in different fields, with reinforcements between their concerns. One of the reinforcements used was z-pinning where its efficacy is closely related to the volume content of pins where a 2% of volume content improved by around 20% and 50% the fracture strength and fracture energy respectively.

2.8 Interlaminar reinforcement: Nonwoven veils

As noted above, one of the major disadvantages of using fiber reinforced composite material is its poor interlaminar toughness. To counteract these effects it is necessary to use interlaminar reinforcements, for this specific work, the use of a specific interlayer reinforcement with fibres randomly oriented known as veils. Studies [99–105] about the effect of nonwoven veils in the improve of mechanical properties of composites show promising results.

Lee et al. in two of his studies [105, 106] researched the interlaminar fracture toughness of composites with non-woven carbon cloths as interlaminar reinforcement, noting a significant increase in Mode I (about 28%) and Mode II (260%). These cloths consisted of small fibres randomly oriented from a range of 3 to 25 mm, distributed in a very thin layer, having a relatively low manufacturing cost. This author [107] also evaluated the composites behaviour with carbon fiber and reinforcement of polyester, glass and non-woven aramid cloths with respect to tensile strength, finding that these cloths decrease Young's modulus and tensile strength but it also reduces the dispersion of resistance data.

Veils can be produced with a very low areal weight (8-20 g/m²) and can be positioned between the dry fabric layers used in the VARTM technique. The movement of these randomly oriented fibers from the position of the intermediate layer to the upper and lower fabric layers during the infusion and curing process gives them the ability to improve interlaminar toughness through fibre bridging. However, the effect of the improvement of the veils depends on different factors, such as the matrix system, the structure of the fibre and the areal weight of the fiber [99, 101].

To address these results, polyphenylene sulfide (PPS) veils are used as modifiers of interlaminar fracture toughness in the research presented in this thesis, evaluating the effectiveness of polyphenylene sulfide (PPS) veils under flexural loads. The effects of the veil parameters, such as fibre density, fibre diameter, veil thickness and the adhesive used to glue the fibers are beyond the scope of this work

and will need to be investigated in future work, because it worked with a single type of veil.

2.9 Final remark

Investigations concerning beams in composite materials have been extensively developed over the past few years by publishing a considerable number of works. Taking this review to the need to observe the experimental progress of different cross section in beams and joints as an essential part of several applications. These beams in composite material supply the need for ultralight structure, highlighting its greatest disadvantage, the same in the base material. To counteract these effects, there are different reinforcement techniques, among which stand out for beams, stitching, z-pinning and tufting, which allow the improvement of properties in out-of-plane directions. In addition, composites allow to serve as a base material, and work as reinforcements where the beams are made of another material, such as steel, aluminum or concrete.

In the next chapter, details of materials and methods used in the experimentation and manufacturing of the structural elements with cross-section I and T are presented.

EXPERIMENT METHOD AND MATERIALS

3.1 Introduction

In this chapter, fiber reinforcements, resin systems and nonwoven veil material that have been used to manufacture the sample of I and T beams are presented. There are currently no standards for specimen dimensions, design of fixture devices and testing procedures. As a consequence, a series of tests and modifications have been carried out, and different equipment designs for the tests were developed to optimize the final fixture configuration. The different beam geometries were manufactured using the VARTM method. Manufactured specimens were purchased from a specialized factory. In the final part of this chapter, mechanical tests used to measure the flexural strength of these beams are presented.

3.2 Materials

3.2.1 Matrix

Two resin systems were used in this project, both being epoxy resin systems without modifications. According to data from the beams manufacturer, this resin was used in the manufacture of the specimens at the standard defined dimensions and represents approximately 50% of the composite material composition. Complementary information appears in the appendices of the work in the purchased beam catalogue.

On the other hand, the resin and hardener used during the reinforcement addition process were supplied by the company EpoxeMex. The resin is an epoxy,

KUKDO KFR-120, and the associated hardener used is a formulated amine, KFH-163. This epoxy infusion system has low viscosity with high mechanical and thermal properties compared to general systems. In addition, due to the 200 minutes for a kilogram of pot life offered by this resin, it is suitable for the manufacture of large elements without the adverse process of excessive viscosity during infusion. This aspect also becomes relevant as this system becomes convenient for different processes, such as resin transfer molding and hand lay-up, which take some time necessary to deal with resin movement and impregnated fibers. The manufacturer's data for the resin and hardener are listed in Table 3.1. The mixing ratio suggested by the manufacturer is 100 parts by weight of resin (KFR-120) to 29 parts of hardener (KFH-163). Some physical data for the mixture appears in Table 3.2, highlighting that the pot life of the resin depends on its weight because the curing reaction is exothermic. The expelled heat during the process increases the temperature of the mixture, accelerating the reaction of curing.

Table 3.1: Resin and hardener specifications.

Components / Properties @ 25°C	KFR-120	KFH-163
Density (g/ml) DIN EN ISO 1675	1.0-1.2	0.8-1
Viscosity (cps) DIN EN ISO 255	1.0-1.5	5-50

3.2.2 Reinforcements

Respect to specimens manufacturing, plain weave carbon fibre fabric was used in the manufacture of I and T structural elements. Carbon fibre is relatively expensive compared to fibre glass, and although the latter has a greater presence in the applications related to the wind energy industry, however, the present work only focus on carbon fibre because the veil has mostly pronounced effects when this fibre is used. Three different orientation of carbon fibre were utilised in this study. Carbon fiber of unidirectional and plain weave of 0°/90° on the upper and lower flanges giving beams a high flexural strength. The use of a fabric with an orientation of ± 45° in the web gives it a better shear resistance, in addition this properly distributes the loads

between the upper and lower flanges. This I-beam configuration was manufactured by the DragonPlate™ company, and such description is shared by the T beams, because this geometry is taken from a symmetrical half of the I-beam. The stacking sequence is presented in Tabla 3.3.

Table 3.2: Processing data for epoxy resin system.

Mixture density (g/ml) DIN EN ISO 1675	25°C	1.0-1.2
Cured density (g/ml) DIN EN ISO 1183	---	1.1-1.2
Mixture viscosity (cps) DIN EN ISO 2555	25°C	200-400
Pot life (min) (23°C, 65 RH) DIN EN ISO 9514	100 g 1000 g	340-360 140-160

Tabla 3.3: Fabrics orientation

Material	Cantidad	Lugar	Estructura	
Plain Weave CF	2	Web	± 45°	
Plain Weave CF	2	Flanges	± 45°	
CF	1	Flanges	0° UD	
Plain Weave CF	1	Flanges	0°/90°	
Plain Weave CF	2	Web and inner part of flanges I+D	0°/90°	An external layer above whole veil to add it

3.2.3 Interlaminar veils

As discussed in section 2.8, nonwoven cloths have been used in composite materials for the purpose of increasing interlaminar fracture toughness. The polyphenylene veil in Figure 3.1 was supplied by the tfp company, highlighting as the most relevant of its characteristics the surface weight, which is 10 g/m².



Figure 3.1: Interlaminar veil.

3.3 Fixture

A cross section T is not a common geometry for test specimens and therefore lacks standards for flexural tests of T beams. As a consequence, the equipment for these tests had to be considered with versatility among design requirements, that is, capable of performing tests for both geometries worked in this thesis, I and T. Therefore, to satisfy this requirement, a series of fixture has been designed and improved, which is presented in the following sections.

For flexural tests on beams, there are two different classes, identified according to the amount of load application points, that is, there are four-point and three-point tests, the basic difference between the two test methods is the location of the maximum bending moment and the maximum axial tensions fibre. Looking for simplicity as another characteristic for the design of the equipment, and also being the most accepted, we opted for the three-point test, according to the scheme in Figura 3.2.

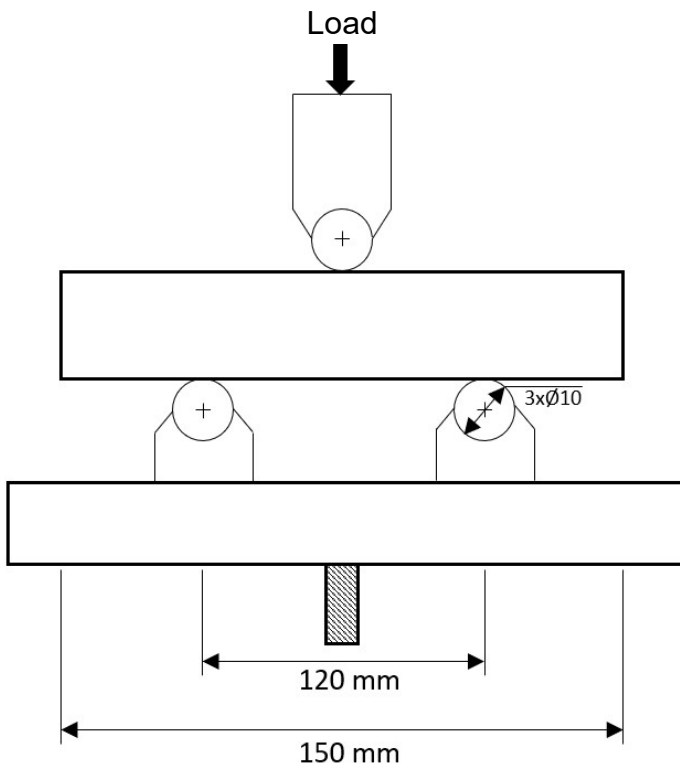


Figura 3.2: Esquema de prueba de tres puntos.

These tests are carried out on flat surfaces in the majority of cases, applying load on the upper surface of flanges and on an upper point in the web for the case of the T beams, and in relation to the beams I, the load is applied along a central line on the upper flange. Both geometries are supported at the bottom in the same way, which is on the flanges, consisting of two equidistant supports from the line of the load application.

3.3.1 First design of test rig

The first design of this equipment was relatively complex. The main objective was to provide the versatility necessary to perform the two positions for testing the I and T beams. The design of this rig consisted of two external sliding parts formed by a fully threaded bar and threaded square rods where the contact rollers were located, which is shown in Figura 3.3. The depth variation of the central part with respect to the other two was limited only by the height of the square rods. There were some aspects against this design that prevented manufacturing, such was the

case of apparent instability when the maximum position required for testing on the T beam was achieved, due to the low presence that would exist between the roller housing and the adjacent walls. Another aspect was the small dimensioning handled, preventing having a larger diameter in the studs and anticipating a possible buckling when loading and having a column behaviour.

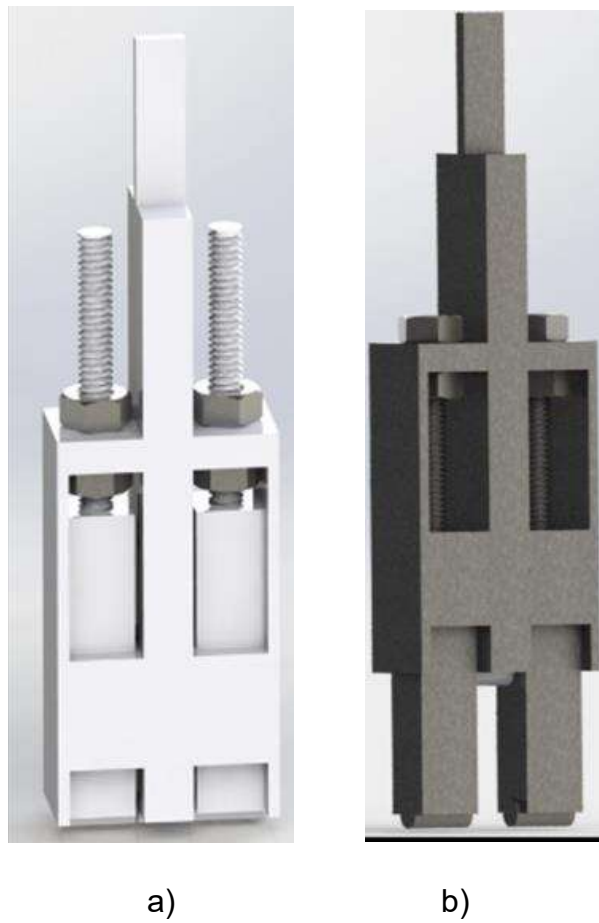


Figura 3.3: First design for test rig in position a) I-beams and b) T-beams.

3.3.2 Second design of test rig

To minimize the associated problems mentioned above in section **¡Error! No se encuentra el origen de la referencia.**, a second generation of test rig was designed. The quantity of pieces was reduced, obtaining a design with greater simplicity for manufacturing, obtaining only one moving part located in the center, leaving the two static, in addition long and threaded parts were eliminated,

handling now just one thread at the joint between a central rod and the host part of the central roller. One of the main advantages is the reduction of instabilities between the different components, because the outer columns where they appear will serve as a precise guide for the central column at all times. There are also three set screws to secure the central rod and allow the handling of multiple web heights in T-beams, in addition to a regulating screw in the central part on the central line. The design presented in Figure 3.4 met all the desired requirements, however, the simplicity of the design was set aside, making another one necessary. Therefore, the design for the team had to be altered again.

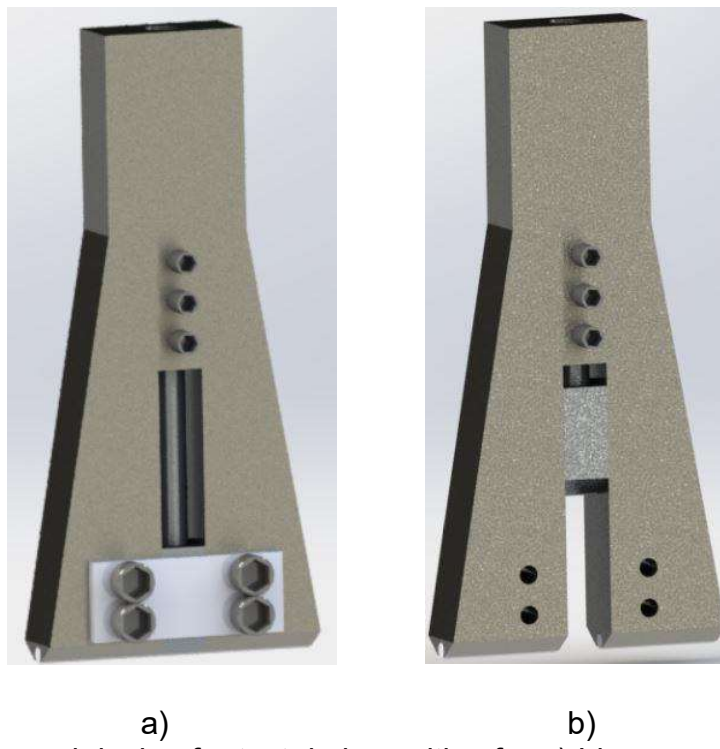


Figure 3.4: Second design for test rig in position for a) I-beams and b) T-beams.

3.3.3 Third design for test rig

Finally, a third design is reached taking into account two aspects forgotten in the previous design, simplicity in manufacturing and versatility for assembly in the universal testing machine. This versatility was translated into thinking about the utility to work with the presence or absence of the grips in the universal machine, due to its complicated handling of releasing this element, the addition of square bars drilled throughout of similar width, allowed upper jaws hold the rig satisfactorily. Another

modification was the suppression of the stabilizer plate of the central rod, because it was considered unnecessary because there were no forces in any direction other than the vertical supported by the little clearance between the rod and the housing channel. Also, the change of section from the bottom to the top would mean an extra operation in the manufacturing process, therefore, an increase in manufacturing costs, so it was decided not to carry out this section change to finally arrive to the final design. An extra rod was used to act as a safe in a possible slide of the central cylinder, showed in Figura 3.5 together with the final design of the equipment.



Figura 3.5: Third design of test rig; a) CAD model, b) manufactured product.

3.3.4 Design of test support base

For the support device design, there were only few design requirements, which were: versatility to support different span length of beams and capacity to be set with grips or without them.

The design was quite simple, which consisted of the elaboration of a sliding channel, where two mobile elements with a threaded hole that allow the insertion of a screw to join with an element that would allow fixing cars with the rail. It should be mentioned that the sliding elements serve as hosts for the rollers required for the test support. In addition, due to the versatility related to the grips, there was a need

to incorporate two removable angles centered at the bottom of the base, as shown in Figure 3.6. The final product of equipment set for testing appears in Figura 3.7.

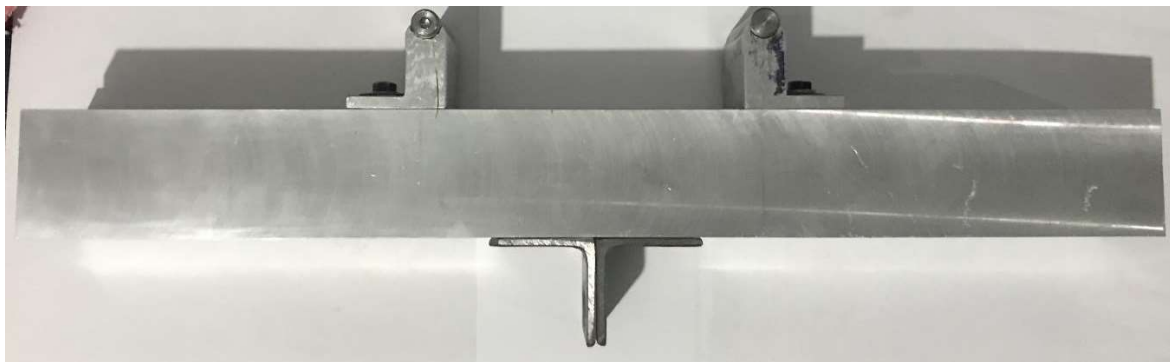


Figure 3.6: Device support for specimens.



Figura 3.7: Final product of test rig.

3.4 Especimens characteristics

The technique used by the manufacturer for the specimens fabrication within this work is resin transfer molding (VARTM).

The length of the specimens was limited to 150 mm due to the amount of minimum required specimens obtained from a total length of 1200 mm. This quantity was distributed as follows: each sample consisted of two specimens necessary to make an adequate comparison between the modified and base beams. Namely, four specimens with I and other four with T geometry were obtained from the total length beam purchased from the manufacturer. Each cross section was distributed as two reinforced and two base specimens as appear in Figura 3.8. The other dimensions that complement the length for the case of the I-beams were: the total height 50.8 mm, 0.965 mm thick, and finally 38.1 mm for the flanges width. The measurements for T-beam specimens were similar to those of I-beam, as they were obtained from a symmetrical cut in half through the web, only the value of the total height was changed by 22 mm.

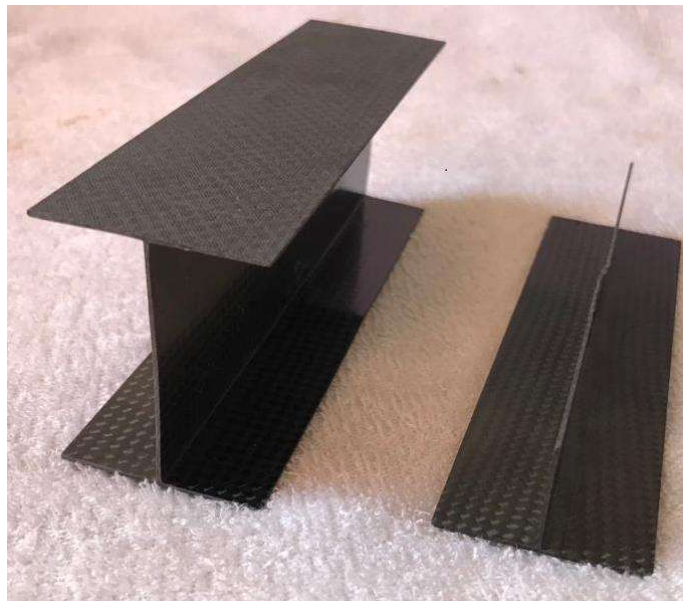


Figura 3.8: Especímenes base con geometría I y T

3.5 Curing and veil characterisation

Once the desired quantity of specimens is had to carry out the tests, the veils and an extra layer of carbon fiber are added, because the usefulness of the

interlaminar reinforcements is precisely as the name indicates it, present between two layers of fibre.

3.5.1 Characterisation of curing time resin

In order to use the epoxy resin system, curing time characterization tests were considered. Always when starting to handle the resin systems, the degassing phase begins, an action that seeks to eliminate the gases resulting from the chemical reaction during the mixing. In the first instance, this phase took longer than usual when altering the weight ratio, around 45 minutes in just 100 grams. Same error was committed, the mixture despite the fact of undergoing a curing phase at 80 °C, the final state was achieved after 12 hours. In a third attempt, the mixing was carried out fixing last errors, however, when the resin was subjected to a temperature at 80 °C, it cured in 6 hours presenting bubbles because the plastic container influence in the curing process. On the fourth attempt, it was decided to change the material of the container with a ceramic one, which due to refractory characteristics prevented the curing of the resin, despite having been at 80 °C for 6 hours. Finally, it was decided to interact by changing the material of the container, and this time the ceramic was replaced by an aluminium basket, allowing a curing with excellent finish with a temperature of 75 °C in 6 hours. Knowing that the resin on average will need 6 hours and a temperature of 75 °C for an ideal cure.

3.5.2 Resin characterisation under tensile tests

To evaluate the effect of the epoxy resin system in stress tests, these ones were performed in specimens composed solely of this system, where the results were used to evaluate the influence in structural performance. The sample is presented in Figure 3.9, and the results of specimens with similar behavior were showed in Figure 3.10.



Figure 3.9: Sample to perform tensile test

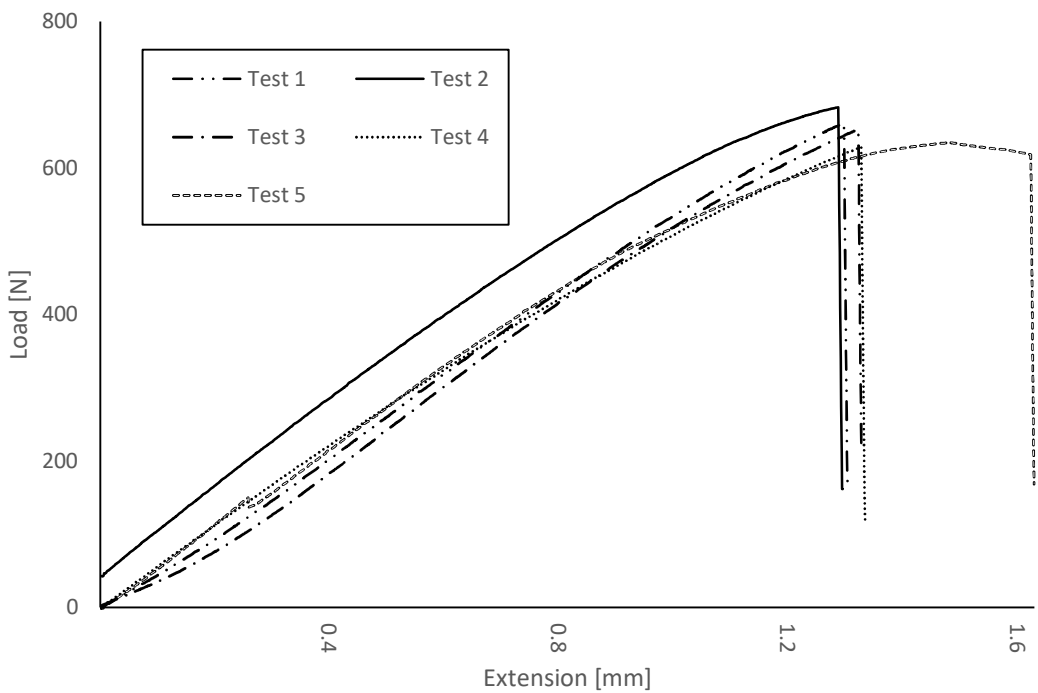


Figure 3.10: Data from tensile tests for resin system.

In the samples with significant data, a failure load value of approximately 650 N was obtained, which, by dividing it by the cross-sectional area of the place where the fault originated, gives the following value for tensile strength:

$$S_T = \frac{650 \text{ N}}{11.5 \text{ mm}^2} = 56.5 \text{ MPa} \quad Ec. (1)$$

3.5.3 Characterisation of veil tensile strength in out-of-plane direction

Due to the lack of data of veils used, performing tensile tests for veils was required. These were conducted by placing the veil between two carbon fibre layers making a sandwich structure, namely, the veil performed the function of interlaminar reinforcement, and also these fabrics were bonded to two steel plates of 25.4 mm and 50 mm dimensions on the surface contact. In a first attempt, the adhesion power of the reaction of the carbon fiber and the resin system to the metal plate was relied upon by not using any release agent, but these first conditions in the experiment resulted in a very early failure, producing the debonding between the interface of the steel plate and the carbon fiber layer.

After the experiment where specimen failed before reaching the desire value, it was decided to apply a bonder agent to delay the failure moment in sample shown in Figure 3.11. This modification allows to increase the strength with respect to the first conditions. However, the failure occurred prematurely again, which occurred in some specimens in the interface between bonder and steel plate and others between fabric and plate. The data to evaluate tensile strength obtained from these two experiments were erroneous, however it increased respect the first attempt and is showed in Figure 3.12. Even though, the experiments did not performe properly, they gave results for a bottom cap for tensile strenght of veil reinforcements. Namely, it exceeds the following value:

$$\sigma_y = \frac{4000 \text{ N}}{25.4 \text{ mm} \times 50 \text{ mm}} = 3.13 \text{ MPa} \quad Ec.\text{ (2)}$$

The previous figure quadruples the value obtained in the first experiment carried out, however, as already mentioned, this barely sets a lower limit of what the veil could support as interlaminar reinforcement.



Figure 3.11: Specimens before and after the test

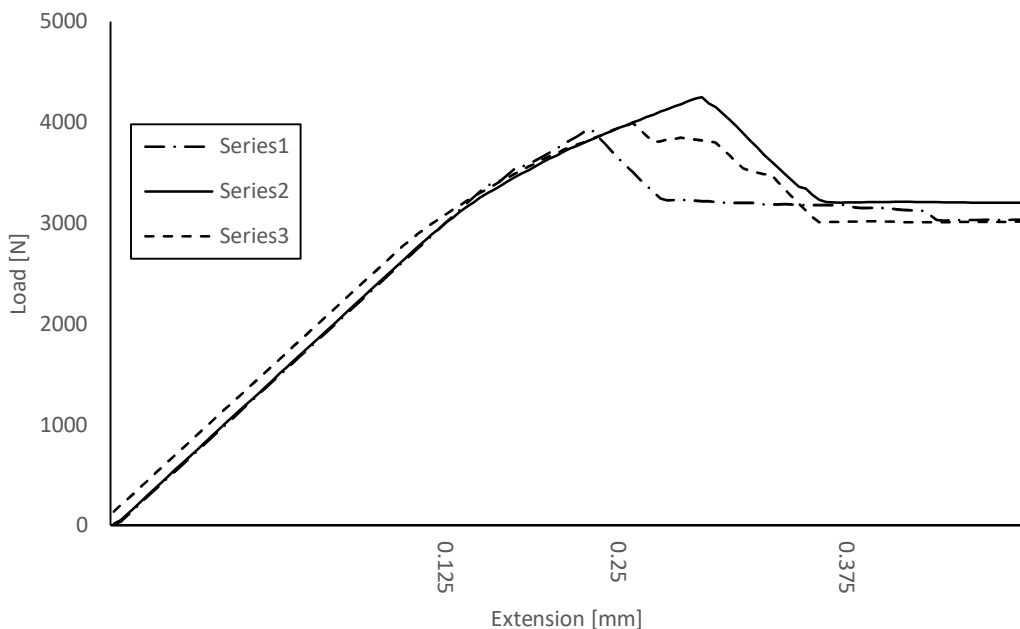


Figure 3.12: Tensile test for PPS veils in out-of-plane direction.

3.6 Veils incorporation

Within this work, the technique used for the addition of veils on I and T-beams within this work is known as hand lay-up. Once the basic specimens consisting of carbon fiber and epoxy resin have been obtained, the interlaminar reinforcements are added together on the materials listed in section 3.2.

3.6.1 Fabric

Being the length of 150 mm for both configurations, and for the I-beam 53.1 mm in height and 19.05 mm in the flanges, the fabric was cut oversized, with at least an extra 10% by each side. The addition of veils is over both sides of the beam web; thus, four veil and four carbon fibre fabrics were cut with rectangular shape and 165 mm x 80 mm as its dimensions. A layer of carbon fibre and veil are placed on each symmetrical side of the beam, which is in the region described with a C as a cross section. A set of one veil and one carbon fibre fabric is positioned by each side for the two I-beams that be reinforced.

For T-beams specimens, one of the dimensions should be reduced by half for the mentioned layers, namely, the fabrics cut for veils and carbon fibre weave will have dimensions of 165 mm x 40 mm being the same amount.

3.6.2 Incorporation process

The use of molds and any other special instrument is unnecessary, except for a brush, Due to the simplicity of the selected manufacturing technique and its predefined shape because of manufactured beams. The appropriate mixture of the epoxy resin system is carried out and then taken to the vacuum chamber to extract as much as possible gases generated in the reaction. A resin layer is placed on the region of interest to subsequently place the veil, digital pressure is exerted to achieve uniform adhesion throughout the surface area. Additionally, once the position and the impregnation of the veil are verified correctly, the following step is putting a resin layer again and positioning the carbon fiber layer. Finally, after pressure is exerted on the fiber cloth to achieve a homogeneous bond, an appropriate amount of resin is applied once again. After performing these steps as seen visually in Figura 3.13, the specimens are placed in the oven for curing process.

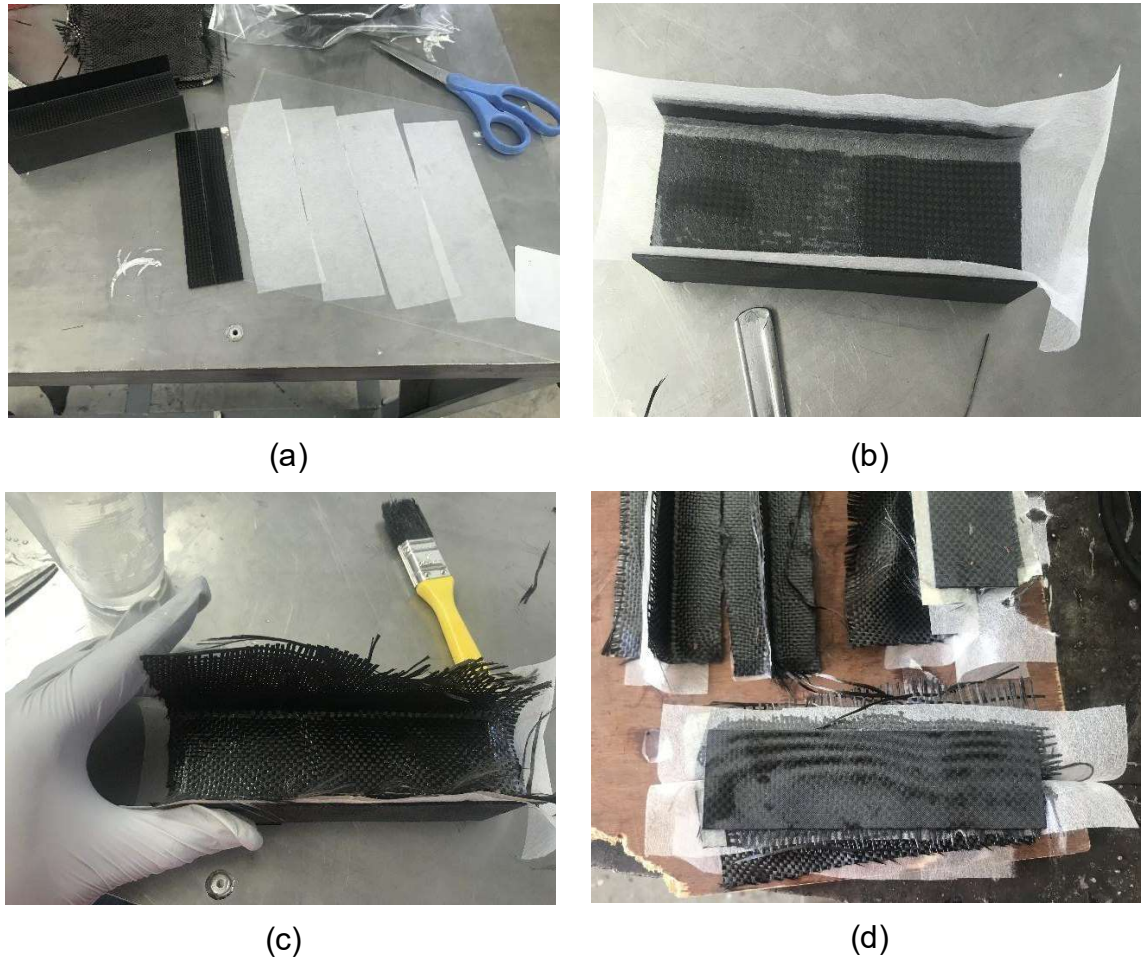


Figura 3.13: Veil incorporation process; a) Resin preparation, veils and carbon fibre fabrics b) veil placement, c) fibre carbon placement, d) specimens after curing process.

3.7 Mechanic characterisation

Flexural tests were carried out on beams with different characteristics to define the maximum load that specimens can bear before failure. As mentioned before, I and T sections are not common geometries in the practice of tests, consequently, there is no standard for the procedure or for the specimens geometry.

The maximum loads measured were below 4 kN or around. The load capacity of the cell of the testing machine was 25kN and according to the manufacturer's guide the reliability is 1% of its capacity.

A series of flexural tests were carried out on specimens with two different configurations, two with interlaminar reinforcement and two unreinforced for each geometry to evaluate the improvement. From the comparison of test results of different specimens, it is concluded that reinforced beams quadruple the maximum load with that they can bear respect to base specimens.

According to the suggestions of different flexural test standards, the test is chosen with a distance between supports of 80% of the total beam length, being 120 mm between them. As regards the thickness in the walls of the web and the flanges, they vary in reinforced specimens possibly due to extra layers addition of carbon fibre to encapsulate the veil. In the web section, the thickness practically doubled, by adding two more layers, leaving a total of four, also if you take into account the thickness of each veil, it increases even a little more than double. Regarding the flanges section, the original manufacture counts with 4 layers of carbon fibre, adding a layer and a veil would increase by approximately one third of the original thickness. The flexural load supported by the beam samples was measured using an Instron 8872 hydraulic test machine with hydraulic grips which held the designed test equipment. The machine was operated in displacement control with a ratio value of 1mm/min on specimens. Load and extension were measured during the tests using the load cell of the machine and the motion sensor, respectively. Failure criteria to stop the machine were not activated, opting to appreciate further details of veil influence.

3.8 Final remarks

- A rig and a support were designed for static tests for I and T beams. The fixture was presented in Figure 3.5 and Figure 3.6. The diameter of the rollers was 10 mm, to avoid applying a high concentrated effort on the specimen.
- The test rig was designed offering versatility in adoption for multiple heights for a T beam, as well as providing ease of installation with the presence or absence of grips in the universal machine.

In the next chapter, the results of the mechanical tests of the sample and explanations of possible reasons that could affect the specimens behaviour.

STATIC TESTS

4.1 Introduction

After having carried out the preliminary steps, where different primary aspects were detailed in the experimental phase, this chapter is written to define what concerns mechanical property related to flexural strength of samples and the effect exhibited of different modifications while the beams were subjected to static mechanical tests.

4.2 Behaviour of base specimens

The base specimens are the control with which the reinforced specimens are compared, both configurations of I-beam are showed in Figure 4.1. The results of the flexural tests of the I-beams sample are presented in Table 4.1, while the results for the sample of T-beams are presented in Tabla 4.2.

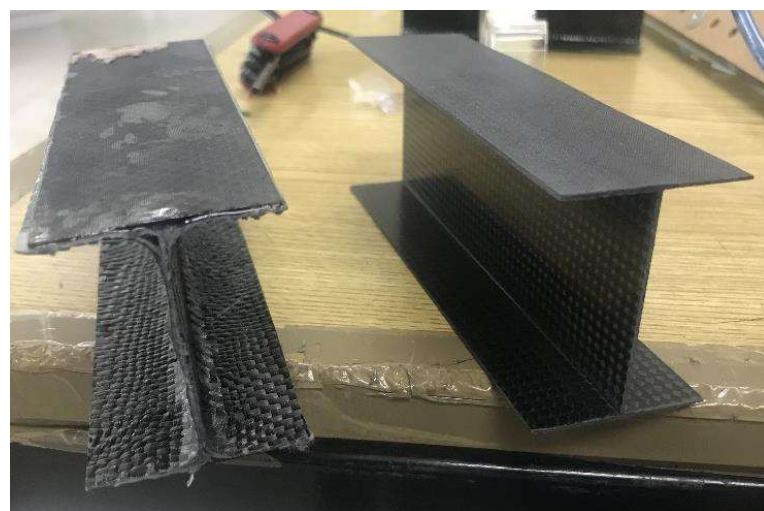


Figure 4.1: Reinforced and base specimens.

Table 4.1: Results of I-beam base sample.

Label	Thickness (mm)	Width (mm)	Web height (mm)	Maximum load (N)	Deflection under maximum load (mm)	σ max (Mpa)
I1	0.965	38.1	50.8	1257.18	2.22	2.398
I2	0.965	38.1	50.8	1259.36	1.85	2.4

Tabla 4.2: Results of T-beam base sample.

Label	Thickness (mm)	Width (mm)	Height (mm)	Maximum load (N)	Deflection under maximum load (mm)	σ max (Mpa)
T1	0.965	38.1	22	470.7	1.29	36.55
T2	0.965	38.1	22	423.44	1.57	32.88

With only two specimens in each sample it is impossible to perform any statistical treatment of the data presented in Table 4.1 and Tabla 4.2. However, a small difference is shown between the I geometry specimens for the maximum measured load, but slightly increased for the T-beam specimens. Regarding deflections where excessive damage occurred, there was a difference between specimens 1 and 2 of both configurations a little more considerable to be in the order of 18%.

The applied load-deflection graphs of the flexural tests for the I and T beams are presented in Figure 4.2. The graph shows that the highest damage to the I beams occurred about 2 mm of deflection on average with a load of 1257 N and after that the initiated crack propagated through the composite material in a disorderly manner, observing that the applied load rises again up to a value very similar to that of failure. As for the T beams, the greatest damage occurred on average at 1.4 mm of deflection with a load of approximately 450N, it is estimated that the crack propagated steadily, due to the plateau during certain extension, then a decrease in the applied load, where it is possibly due to a breakdown of fibres from a larger area falling back to another plateau.

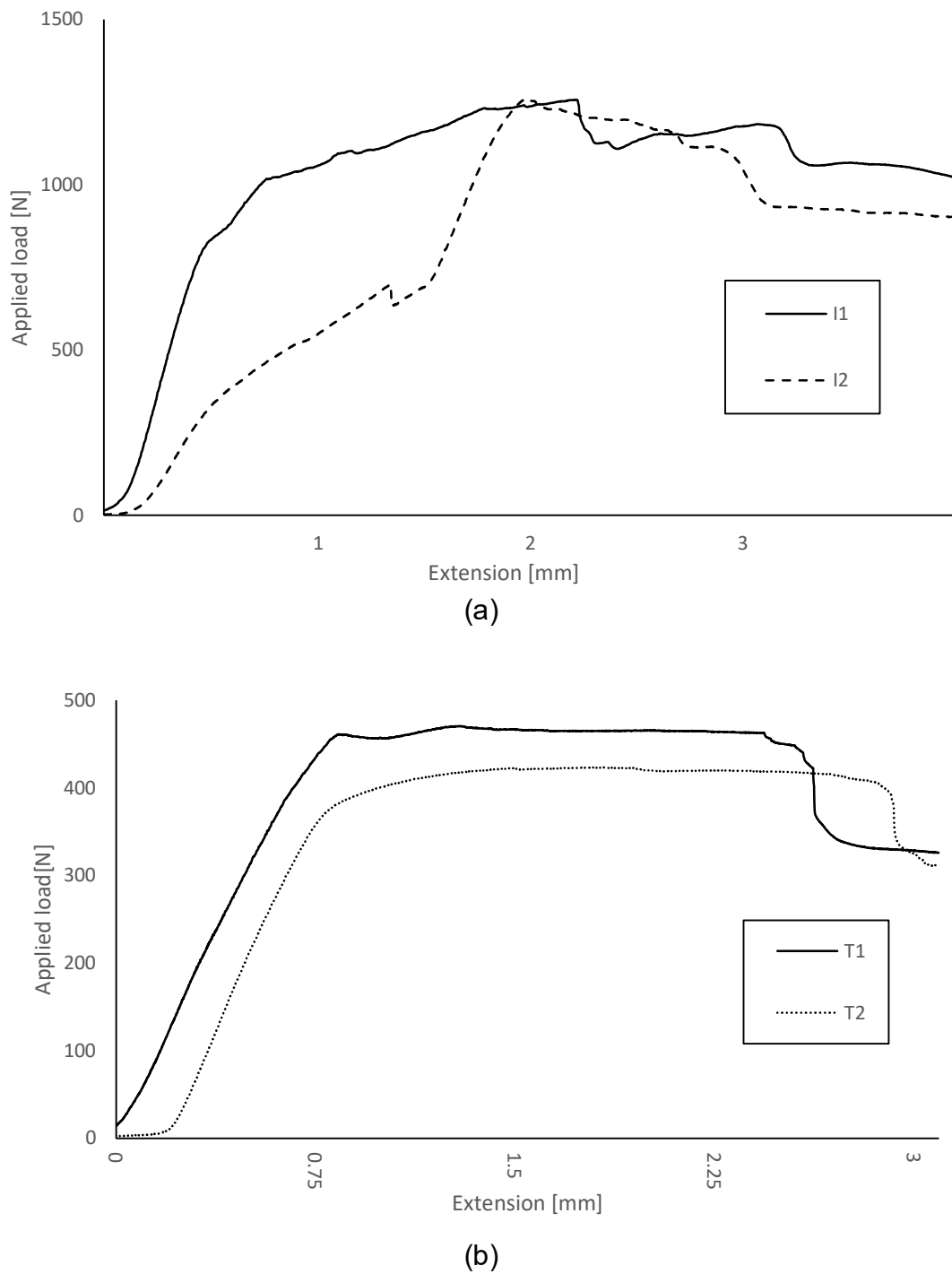


Figure 4.2: Results of base specimens; a) I geometry, b) T geometry.

4.3 Reinforced specimens with PPS veils

The dimensions and maximum load values applied to the beams containing polyphenylene sulfide veils, on flanges and core, are presented as follows: Table 4.3 for I geometry and Table 4.4 for T geometry. Again, the possibility of a statistical treatment is null, due to the small number of specimens, as a consequence, only the difference between one test and another is taken into account, which in the case of I beams, is considerable, being in the order of 16% in the maximum load data, there is an average value of 3.8 kN. While for T beams, the difference between the two maximum loads recorded was relatively small, generating an average maximum load of 1.68 kN.

The graphs of load applied against deflection of beams containing polyphenylene veils are presented in Figura 4.3. Around 1.23 mm of deflection, the I-beam presented crack initiation, without being very well defined, however, as regards the T-beams it allows to appreciate in detail an irregular signal, namely, a small 1.25 mm drop in height. The maximum applied load occurs at a deflection of 7,614 mm for RI1, and for RT1 shortly after 2,365 mm of extension falls suddenly, probably due to the breakage of fibres in the I and T specimens.

Table 4.3: Results of I-beams for flexural test.

Label	Flanges thickness (mm)	Web thickness (mm)	Width (mm)	Web height (mm)	Maximum load (N)	Deflexion at the maximum load (mm)
RI1	1.46	1.96	38.1	50.8	4151.86	7.614
RI2	1.46	1.96	38.1	50.8	3493.02	3.689

Table 4.4: Results of T-beams for flexural test.

Label	Flanges thickness (mm)	Web thickness (mm)	Width (mm)	Web height (mm)	Maximum load (N)	Deflexion at the maximum load (mm)
RT1	1.46	1.96	38.1	22	1728.99	2.365
RT2	1.46	1.96	38.1	22	1630.16	1.755

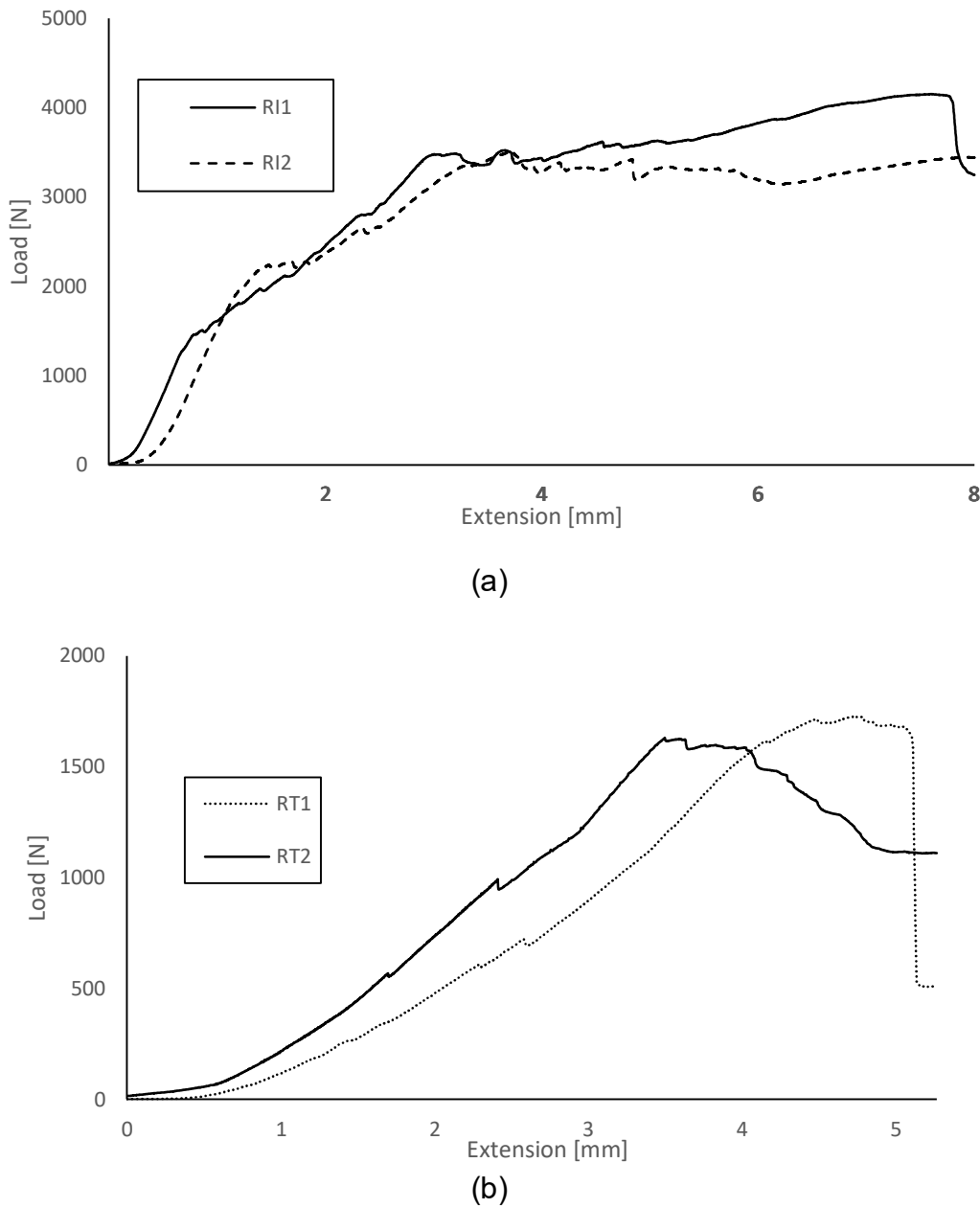


Figura 4.3: Results of reinforced beams; a) I geometry, b) T geometry.

4.4 Discussion

The results of the flexural tests of the base and modified specimens in I and T geometries are presented in Figura 4.5. As can be seen, the addition of interlaminar reinforcement increases the limit of the maximum supported load by up to 400% in both geometries. It is estimated that during the tests the first signs of crack initiation

appeared in the curved section of the beam, namely, in the triangular volume of the joint between flanges and web. Although the veil does not directly affect this area, when a minimum space is noticed after the curing process, there should be some benefit in the veil interacting with other carbon fiber fabrics.

The increase in the flexural load withstood is due to fibre bridging triggered by veil distribution in a fabric from flanges-web-flanges. However, other factors come into play when trying to estimate causes for the increment in load, one could be the fact of having added extra layers of carbon fiber, two in web section and one for each flange. Even though a linear relation would exist between supported load and section thickness, a maximum increase of twice could be expected.

Displacement comparisons when maximum load occur show a significant improvement for reinforced structures, showing an increase of 55% for T beams and 177% for I beams, however there was no bending in either of the two configurations for I-beams due to the reduced distance between supports. In addition, this affects the behavior of a beam where only buckling occurred as can be seen in Figure 4.4.

Another relevant aspect is the effect of the modifications in beams in the extension of the damage produced in the web, concluding that the specimens with less damage in the web are those that were able to bear a higher load.

Regarding reinforced beams behaviour, despite the fact that the maximum supported load increased significantly, sometimes there are other variables that are important, such as damage tolerance, seeing Figura 4.5, in one of the reinforced I-beam, the supported load falls sharply after reaching the maximum peak while in the other specimen, the load remains constant but with small fluctuations, if compared with the base specimens, this base beam behavior is preferred for a structure. Something different happens with the reinforced T beams, once they reach their maximum peak of supported load, one has an abrupt decrease, but manages to stabilize immediately afterwards in a range similar to the base specimens, while the other decreases the ability to support load gradually and tends to stabilize with a little more than twofold supported load by the base beams.

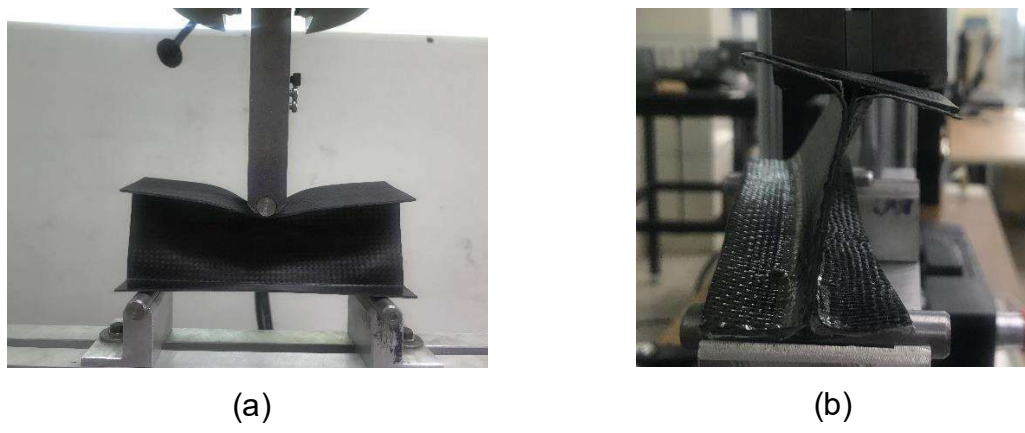


Figure 4.4: Test in I-beams without bending, a) base specimen b) reinforced specimen.

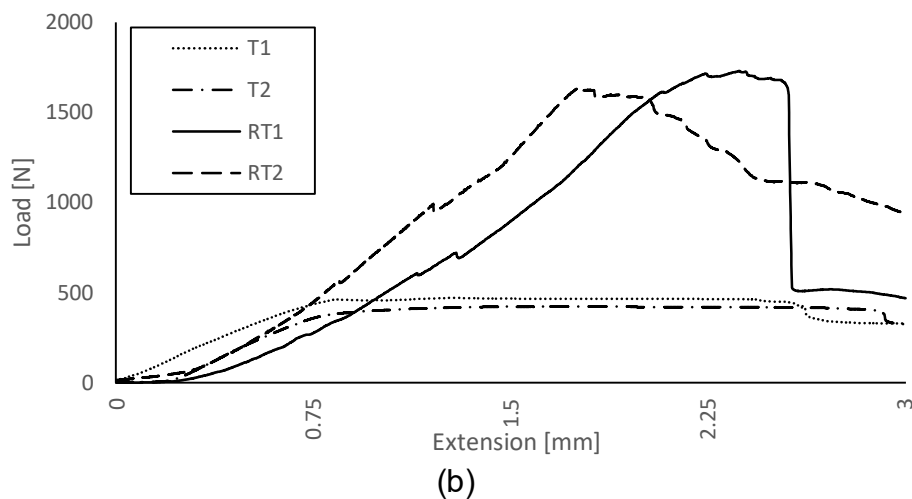
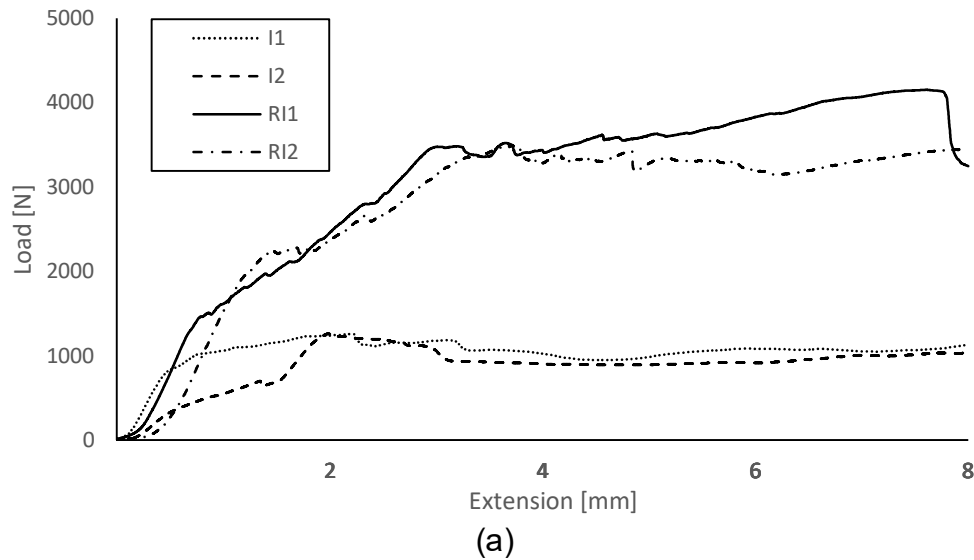


Figura 4.5: Comparison between base and reinforced; a) I-beams, b) T-beams.

MODELING BY THE FINITE ELEMENT METHOD

5.1 Introduction

A finite element model was developed to analyse the distribution of stresses in composite beams and identify stress concentration points in the structures. The model also provides a deeper understanding of present stresses present in the beams.

5.2 Modeling of I and T beams

In order to predict the structural element behavior with I and T cross-section, which is subjected to a flexural test with 3 contact points, it is necessary to perform a modeling using the finite element analysis (FEA).

5.2.1 Geometrical modeling

To model the structural elements, two options were available, which consisted of using specialized CAD software or modeling directly from the Finite Element software ANSYS APDL. It opted for the latter, due to the apparent disregard for the measures system and possible problems that sometimes arise from models importation from other software, in addition, the geometry lacks very complex configurations. As an initial step, the parameters are stipulated to define the two quarters of the cylinder as solid volume with radius $r = 1\text{mm}$ in the software interface that will represent the rounding section in the joint of web and flanges, to then proceed with the elimination of volumes, and leaving only the areas and other

defined geometric subtleties necessary for the creation of areas. Next, working in the web part, where the points of interest keypoints are defined in the YZ plane necessary to proceed with the subsequent creation of lines. Then, we proceed to define the areas corresponding to flanges, again from the creation of points of interest keypoints, this time in the XZ plane, and subsequently, establishing lines that connect the points correctly. If the first option would have been selected, referring to the use of specialized CAD software, these steps would have been simpler, to the point of having of having created surfaces and then importing the model from the software CAD to ANSYS APDL with an extension called * IGES. Figure 5.1 shows the representation of the geometrical models defined only the contour with lines to work in ANSYS.

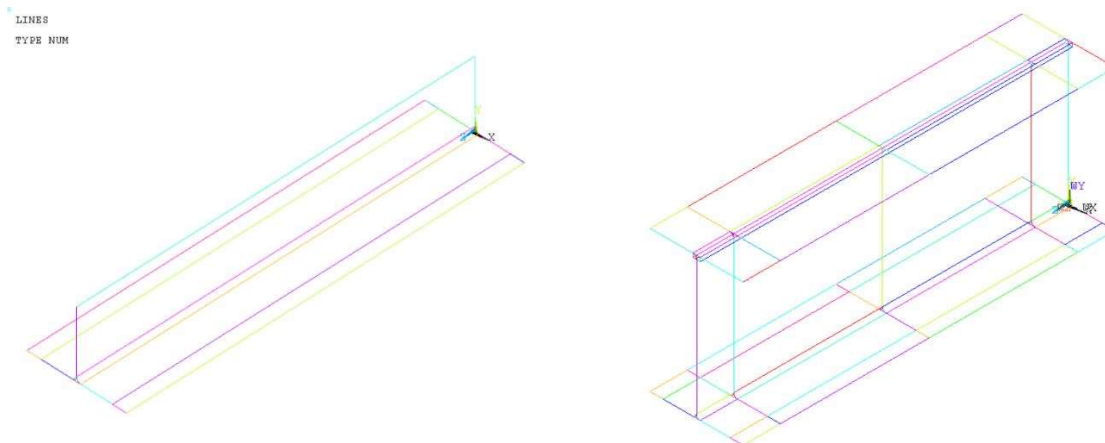


Figure 5.1 Lines in geometrical models de las vigas I y T.

When defining the model in keypoints, lines in planes of interest and areas of curvature, we proceed with the definition of the missing areas in web and flanges, from the use of the corresponding function for the areas creation based on the surrounding lines. This process is carried out because these surfaces are flat and, therefore, represent ease when generating them, an inverse process to that used to create areas of smoothing.

As a first attempt, subareas were created on areas corresponding to flanges, which were going to be necessary for the generation of a configuration called ply

drop-off [108], which detailed a gradual section change for layers in the composites, yet due to the high ratio of dimensions between thickness and flanges width it was not feasible to make such an adaptation. Figure 5.2 shows I and T beams fully defined in areas and the lines that delimit it, finally establishing a complete geometrical model that is used as a reference for the analysis by the finite element method.

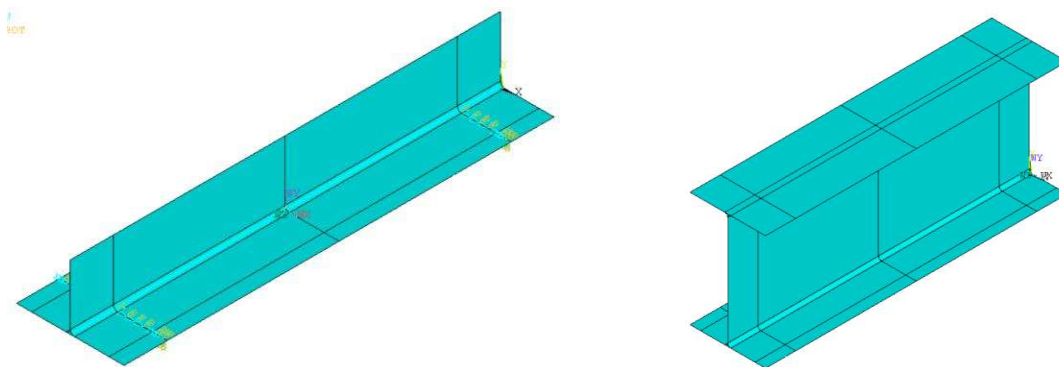


Figure 5.2: Area in geometrical models for FEA in I and T beams

5.2.2 Materials

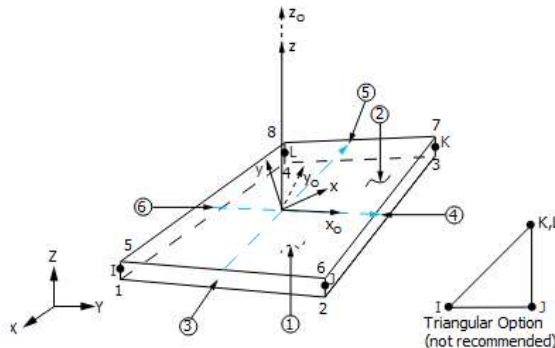
In order to complete the modeling in the finite element software, it is essential to take into account the materials selected for the specimens manufacture, and to insert this information in the corresponding section. In this task a number was assigned to the carbon fiber, a reference nomenclature necessary to successfully establish these properties for each element in a later step. All the materials defined in the process are used for a structural analysis, linear analysis (small deformations) and elastic behavior, showing the summary of the materials in Tabla 5.1.

Tabla 5.1 Material for FEA model of beams

No. Mat	Descripción	Tipo
1	Fibra de carbono	Elástico-ortotrópico
2	Resina epoxica	Elástico-isotrópico

5.2.3 Elementos

For the modeling in finite elements of the beams, the element called Shell 181 stands out, being a mathematical model that serves to analyse structures of thin to moderately thick, commonly called shell. It is an element of four nodes with six degrees of freedom in each one: translations on the x, y, and z axes, and rotations around the x, y, and z axes, to which several layers with different orientations can be assigned. Namely, a stacking sequence to start the arrangement of layers according to what was manufactured, from the bottom, from the top, or from the middle plane generating symmetry, being ideal to match successfully between layers coming from another section. This element can be used in triangular and quadrilateral shapes, offering better performance in the latter geometry (Figure 5.3).



x_0 = Element x-axis if ESYS is not provided.

x = Element x-axis if ESYS is provided.

Figure 5.3: Element description "Shell 181".

Due to the nature of the "Shell 181" element, the creation of real constants was not possible, therefore, the generation of sections where the thickness showed a varying value due to the amount of layers used is impossible to automate. The generation of the stacking sequence of layers is the next step to the definition of material and type of element, in addition to varying aspects with respect to the area where the stacking will be set, whether it is web, flanges or the smoothing area.

Se posee espesor constante en todas las capas y a lo largo de todas las dimensiones de la viga, sin embargo, el manejo del apilamiento a lo largo de las diferentes regiones se hace indispensable, debido a que existe una bifurcación

proveniente del alma y, por consiguiente, la sección del redondeo solo cuenta con 1 capa cada región, sumando en total 2 capas provenientes del alma y que serán 4 en la sección de los patines. Cada capa en total, es decir, con resina y curado el material compuesto, se estima un grosor de 0.45 mm seleccionado de la teoría existente y de especificaciones de fábrica.

There is constant thickness in all layers and along all the dimensions of the beam, however, the handling of the stacking sequence along the different regions becomes indispensable, because there is a division coming from 2 layers in web and, consequently , the rounding section only has one layer each region, however, it will be four in the flanges section. Each layer in total, with resin and cured composite material represents a thickness of 0.45 mm obtained from the physical specimen.

Another indispensable element for the analysis by finite elements of this beam was the element “SOLID 185”, an element with mathematical model that, contrary to the one defined above, it bases its work on the three-dimensional modeling of solid structures, in addition to being an element with reduced complexity for its solution, only being defined by eight nodes, having three degrees of freedom in each node, translations in the nodal directions x, y, and z (Figure 5.4).

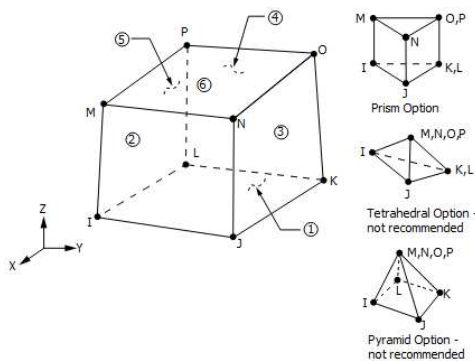


Figure 5.4 Element description "SOLID 185".

This element was selected exclusively to analyse the volume present between the rounding sections of I and T beams, specifically, in the prismatic volume present at the junction of web with flanges, where the characteristics of the epoxy resin are used to simulate the existing material in this area.

5.2.4 Mesh

Once the division of the areas of interest, the allocation of material and the stacking sequence of the layers for different configurations, the mesh generation process is carried out. Elements are generated in the areas using the “mapped” tool in the case of skates seeking to have as homogeneous geometries as possible, setting as a parameter a size of 5 mm for each element, although this is an approximation, since the software defines the ideal size. The ideal element type is selected, as well as the stacking sequence according to the region of interest. Four stacking sequences were defined to obtain an accurate splicing between layers, it should be mentioned that the thickness of the layers was defined as 0.45 mm. The first one was assigned to the soul and consisted of two $\pm 45^\circ$ layers with a medium plane, then the sequence for the smoothing area with only one $\pm 45^\circ$ layer appears, starting from the bottom. The third sequence was created for skates of the form $\pm 45^\circ, 0^\circ \text{ UD}, 90^\circ$ with a offset of 0.45 mm to set alignment with the layer coming from rounding. Finally, the fourth sequence used for the lower surface of the prismatic volume existing at the junction of the flanges and web with the same sequence as the previous one, but with a start from the bottom. After this allocation the volume is meshed with solid 185 in automatic mode to allow the software to successfully join the nodes coming from the surrounding areas.

Figure 5.5 shows the final general meshing achieved in the two beam models, having homogeneous element geometries, in addition to be a symmetrical mesh with respect to the YZ plane.

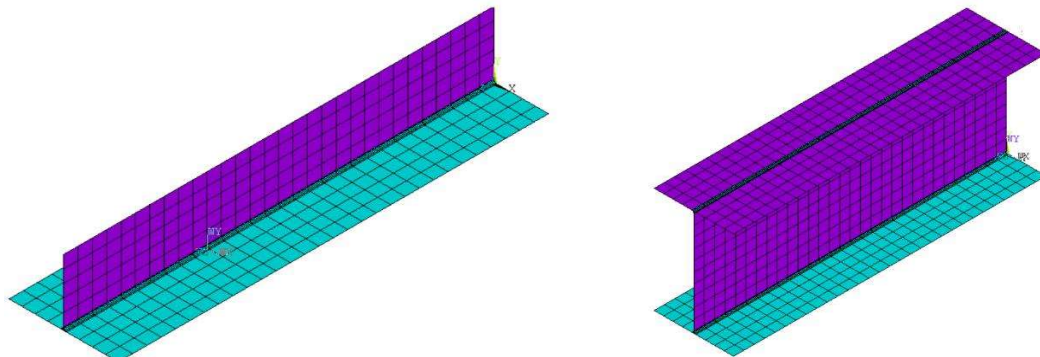


Figure 5.5: General mesh of models

It should be mentioned that the different colours shown in the figure are related to vector normal to area. A purple area will have the normal direction opposite to the blue areas. It is for this reason that the importance of the orientation of the elements becomes vital because the mechanical properties established through the material must be in correspondence with the global system of model so that the elements are required to behave as it was established by the proposed model.

Figure 5.6 shows the cross section of the beams and the staggering achieved with the different stacking sequences.

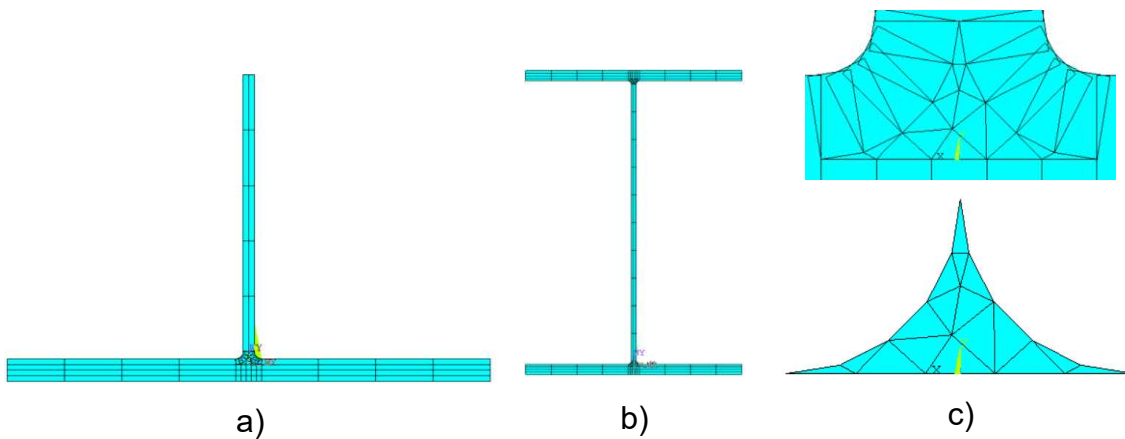


Figure 5.6: Stacking sequence as beams thickness; a) T-beam, b) I-beam, c) epoxy resin volume.

At this point there is a model ready to continue with the following steps as they are: the definition of load conditions and body constraints.

5.2.5 Boundary conditions

The flexural test to which the real model will be subjected consists of three points, that is, two rollers that will serve as support for the specimen and another that will apply the load. To achieve a simple finite element model, the approximation of idealizing the support rollers as geometry lines was used, restricting them in the following way:

$$u = 0 \quad v = 0 \quad w = 0$$

$$\text{Rot } y = 0 \quad \text{Rot } z = 0$$

Only allowing rotation on the x-axis, waiting for the bending phenomenon to act freely on the model.

5.2.6 Load

The applied load will only be in vertical direction, positioning in the middle along the x-axis length, more precisely on nodes of the mesh and simulating the action of the pusher roller. The load value will be the maximum data supported by the physical model during the bending test before the failure. Therefore, the loads will be defined with the following values:

$$\text{For } T - \text{beam: } P = 1258 \text{ N}$$

$$\text{For } I - \text{beam: } P = 450 \text{ N}$$

5.2.7 Postprocessor

In this phase the analysis of the models in FEM is carried out, where the results of the solution previously made by ANSYS are obtained. The data of interest in this analysis are the stresses in the Y and Z-direction, in addition to the indexes of the Tsai-Wu failure criterion. This criterion dictates that, if the index is closer to one, the probability of failure will be very close to occur, it is also vitally important to identify the area where the greatest effort is located, and analyse deeply the volume which only contains epoxy resin. The results are listed below in Table 5.2 in order to observe the criticality.

Table 5.2: Stresses and Tsai-Wu index for beams.

Geometría	Esf Y (Mpa)	Esf Z (Mpa)	Esf YZ (Mpa)	Índice de Tsai- Wu	Deformación
I	-199.90/41.30	-69.12/37.66	-134.18/134.18	0.99	0.07
T	-45.25/58.23	-100.80/57.40	-79.80/80.17	0.99	0.26

According to the Tsai-Wu indices obtained, it is stated that, at the time of loading, any of the geometries are very close to the failure or have already failed, this due to the proximity to one in this criterion.

Evaluating extensively, the region where the maximum value of Tsai-Wu index was located was the prismatic volume located at the web-flanges junction, therefore, the detail will be shown in Figure 5.7. As can be seen, the maximum index is presented in the region where the greatest damage is inflicted, just where the central roller acts in the case of I-beams, or in the middle of the same line of action for the T beam. Another important observation is referring to the indices obtained in I-geometry, since the value displayed for the volume separately is not the same as for the entire specimen, since for the complete geometry a general calculation is estimated, giving support to the epoxy material, decreasing this index.

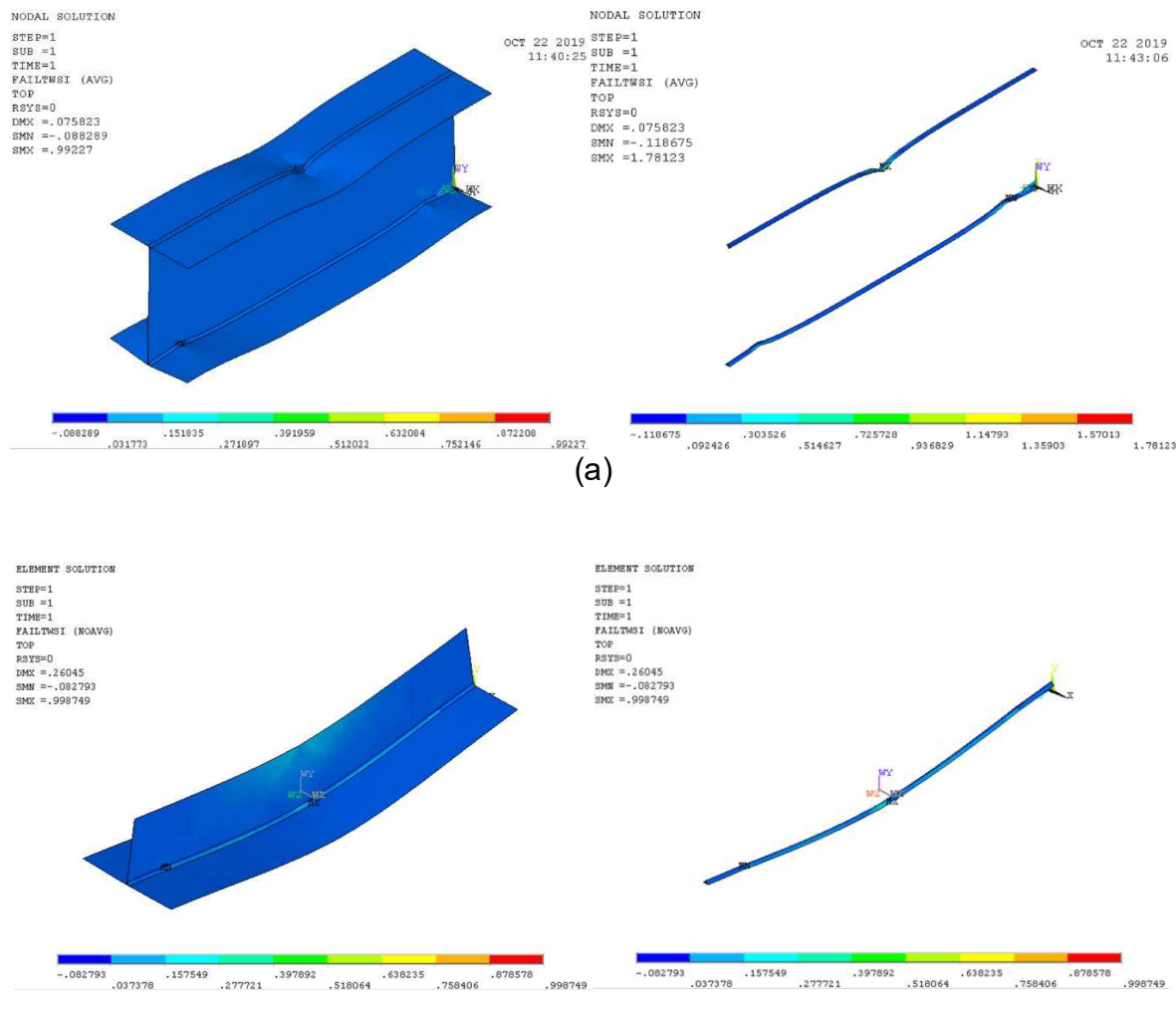


Figure 5.7: Tsai-Wu indices for the whole model and the region made by resin; a) I-beam, b) T-beam.

CONCLUSIONS AND FUTURE WORK

6.1 Conclusions

A protocol for static flexural tests has been developed, because in the literature review there were no standardized methods to perform mechanical procedures on I and T beams of composite materials. Therefore, there were no set dimensions for specimens, application equipment, or parameters such as the thrust speed of the load applicator.

To overcome this condition, certain ASTM standards were used, from which some data were obtained such as the percentage of the distance between supports with respect to the total length, application load speed and contact rollers diameter. In addition, the rig test for the application for specimens in mechanical tests was designed to provide utility to I and T configurations, was designed and developed as part of this research work.

It was found that the introduction of the polyphenylene sulfide veil (PPS) to the specimen gives an increase in the capacity to withstand bending load, showing a quadruplicate value when compared to the base specimens of both geometries. However, this modification affected the thickness of web and flanges with respect to the base specimens, because each veil needed a layer of carbon fiber to be fixed, offering this extra layer somehow some improvement in structural performance . According to the studies carried out in modeling by finite elements, it is observed

that the weakest zone is the one that does not add any value to the structural foundation, namely, volume made solely by resin.

6.2 Future work

- The definition of the effect of the veil parameters on the performance of the beams. Parameters such as areal density, thickness, fiber diameter are characteristics that can influence the performance of the veils. In the literature reviewed for this work, few articles relate these parameters to the mechanical properties of composite materials among their studies.
- Development of a more extensive FEA, where you can obtain experimental data for the veil that allows you to include it in the analysis and obtain satisfactory results.
- Develop longer specimens in order to see the performance of reinforcements in the bending phenomenon for I-beams.
- Interact with the insertion of veils without altering the total thickness of the beam, rather than the value of the thickness of the veil, that is, handling the same number of layers.

MANUFACTURER CATALOG FOR I AND T-BEAMS

DragonPlate™
Material Specifications

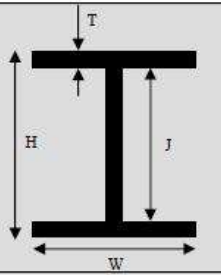



Carbon Fiber I-Beam

DragonPlate carbon fiber I-beams are extremely strong in bending and shear loading. The combination of uni-directional and 0°/90° plain weave on the top and bottom flanges give the I-beam its high bending strength. Utilizing a 45° orientation in the webbing allows the I-beam to have exceptional shear strength, as well as properly transmitting loads between the top and bottom flanges. DragonPlate's I-beam construction allows for an extremely thin, lightweight I-beam to obtain the same effect as a thicker, heavier extruded I-beam. Carbon fiber I-beams can offer similar properties in bending and shear as sandwich panels with the same thickness, but without the added weight from unnecessary core material. Textured finish on the top and bottom of I-beams make for bonding to thin panels to create an extremely stiff and strong structure.

STANDARD SIZES				
J	T	H	W	WEIGHT (lbs/ft)
1"	0.038" ± 0.015"	1.08" ± 0.015"	0.75" +0.125"/-0	0.06
2"	0.038" ± 0.015"	2.09" ± 0.015"	1.50" +0.125"/-0	0.11

Lengths: 48" or 24" (-0, +.25) Finish: Web: Matte
Flanges: Matte Inside
Textured Top/Bottom



Additional Options

- Custom Lengths
- Custom Flange Lengths
- Custom Web Lengths
- Custom Thicknesses
- CNC Machining
- Design and Engineering Services

TECHNICAL SPECIFICATIONS

Properties of Carbon Fiber
Tensile Strength: 512 ksi
Modulus of Elasticity: 33.4 msi

Properties of UNI Fiber
Tensile Strength: 640 ksi
Modulus of Elasticity: 34 msi

Resin
Epoxy resin that accounts for approximately 50% of the composition

$W_f \approx 50\%$

Lay Up Schedule
Web: 2 layers of ±45° plain weave CF
Flanges: 2 layers of ±45° plain weave CF, 0° uni-directional CF, 0°/90° plain weave CF

PAPER PUBLISHED IN CONGRESS

MEMORIAS DEL XXV CONGRESO INTERNACIONAL ANUAL DE LA SOMIM
18 al 20 DE SEPTIEMBRE DE 2019 MAZATLÁN, SINALOA, MÉXICO

Tema A2 Manufactura y Materiales: *Materiales compuestos*

"A review of the experimental progress of composites beams as light-weight structures and their in and out-of-plane properties"

Hortúa Diaz Omar Camilo^a, Ramirez Elias Victor Alfonso^a

^aUniversidad de Guanajuato, Carretera Salamanca–Valle de Santiago km. 3.5 + 1.8 km, Comunidad de Palo Blanco, Salamanca, Gto, CP 36885, México

*Omar Camilo Hortúa Diaz. Dirección de correo electrónico: oc.hortuadiaz@ugto.mx

RESUMEN

Este trabajo revisa distintos estudios acerca del progreso de las propiedades mecánicas y los refuerzos interlaminares dentro de las secciones estructurales primarias: viga I, viga T y unión T hechas de compuesto FRP. Propiedades longitudinales, fuera del plano, flexión, fractura, tensión, compresión, tenacidad y comportamiento de delaminación son reportados y llevan a identificar similitudes y diferencias, consecuentemente, obtener el conocimiento para la configuración óptima para estas estructuras y discutir la viabilidad del uso como estructuras ligeras sugiriendo campos donde más investigaciones son requeridas. Existe una similitud en como refuerzos interlaminares afecta las propiedades mecánicas y una pequeña diferencia entre el z-pinning y el stitching. Sin embargo, los efectos producidos dependen de la variedad de factores, incluyendo el tipo de material, lugar de aplicación de la carga y condiciones de refuerzo. Se propone futuros trabajos basados en los refuerzos que no están siendo estudiados y son puntos críticos de falla.

Palabras Clave: Junta en T, viga I, viga T, compuestos FRP, estructuras ultraligeras

ABSTRACT

This paper reviews several studies about the progress of mechanical properties and through-the-thickness reinforcements into the primary structural sections, I-beam, T-beam and T-joint comprised of FRP composites. Longitudinal, out-of-plane, flexural, fracture, fatigue, tensile, compressive, stiffness properties and delamination behaviour are reported and lead to identifying similarities and differences, hence, to obtain the knowledge of the optimum configuration for these structures and discuss the viability of the use as light-weight structures and suggest the fields where further researches are required. Many studies reached similar conclusions, whereas there is a similarity in how interlaminar reinforcements affects the mechanical properties and a slight difference between z-pinning and stitching. However, the effects produced depend on a variety of factors, including the type of composites, place of the load applications, and reinforcing parameters. Future work was proposed based on the reinforcements that are not being studied and critical points of failure.

Keywords: T-joints, I-beam, T-beam, FRP composites, light-weight structures

1. Introduction

The need for new materials that combine low weight and high toughness was recognised in the '50s as a precondition for ultralight-weight structures [1]. These two characteristics were the main drives to contemplate the use of composites materials, which are material with high specific stiffness and mechanical resistance among several industries such as automotive, thermal, aircraft and optical [2–5]. This latter uses this type of materials with interest in

dimensionally stable ($5\text{--}10 \text{ kg.m}^{-2}$) and large (0.5–2 m) mirrors [6, 7].

The ultralight-weight structures are also used in the energy industry for an easier installation of support towers for the transport of electrical energy [8]; this improvement is beneficial when installing on-shore energy transport. Its application in wind energy enables the generation of clean energy [9, 10] which does not conflict with other land uses

but adversely affect with noise pollution and the intermittency of the wind [9, 11].

Platts proposes a greater participation of composites material in the wind energy, including them in the highest towers found in the offshore farms, while decreasing the corrosion and fatigue to which they are subjected to [12], however, composites are currently only present in turbine blades where can be seen as cross-sectional beams in I and T shapes. There is also an aspect that plays against, which is the high cost of corrective maintenance due to unexpected failures. They are presented mainly in blades, which is attributed a 13.2% of failures of all wind turbines in Sweden [13], and one of the highest causes of failure in the wind industry in Germany [14], expressed in other figures, only applies a ratio of 1 failure/turbine per year (Figure 1) [15, 16].



Figure 1 - A failure occurred in a turbine blade made of composite [17]

Fibre-reinforced thermoplastic related materials are the most suited for light-weight composite structures. However, there are some composites which work with bamboo strips as natural fibres [18]. Other benefits such as mechanical resistance, energy absorption capability, corrosion resistance and cost reduction in manufacturing are pursued with these structures [10], particularly when they formed in the shape of a structural member such as a channel or I-beam [19, 20]. For example, some patented plates report to safely carry 41.600 lbs with a thickness of 2" over a span length of 4ft [20].

Although sandwich composites are ultralight-weight structural materials, they are not as widely used because their resistance in the out-of-plane direction is less than 10% their in-plane equivalent [21] and they frequently fail when subjected to elastic buckling stresses [2, 22]. The honeycomb core stands out; however, as truss cores offer more significant advantages due to it is an open structure [23]. On the other hand, a structure called biomimetic tendon-reinforced improves the out-of-plane properties up to 300% than its equivalent in aluminium [22].

In the case where the thermal stability is a design factor, structures made with carbon-carbon composite material is the first option because its coefficient of volumetric expansion is close to zero ($30 \times 10^{-6} / K$) [1].

Such light-weight structures are mainly present in the advanced materials industry. However, these usually come

from minimum structures such as beams or joints with dimensions and cross-section geometries standardised, for example, T-joints and I-beams. As a result of the prior researches works, high specific strength and reduced maintenances can be found among their characteristics.

This paper focuses on broadly reviewing studies on the progress of mechanical properties and reinforcements in the primary structural sections comprised of FRP composites. The composites which have been investigated include those which are laminated and others which are manufactured through pultrusion technique, and mechanical properties include tensile, compressive, flexure and fracture strength. The review of these researches can lead to identifying similarities and differences in terms of properties mentioned beforehand, stiffness and delamination and hence to obtain the knowledge of the optimum configuration of these structures. This review will also find fields where further researches are required. With the present investigation will be discussed the use of these basic structures as a light-weight structure.

2. Beam Composites

There are two preferred methods for the manufacture of composites beams, the most used and the most economical is the pultrusion process [24–29], which consists in handling fibres as fabric, being wet with resin and then pulled through a die to finish with a curing and a cutting step (Figure 2)[30].

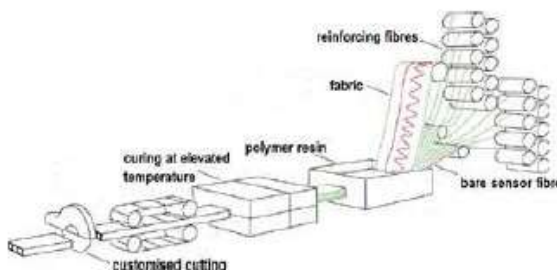


Figure 2 - Pultrusion process [31]

Another technique highly used is VARTM used for laminated beams (Figure 3).

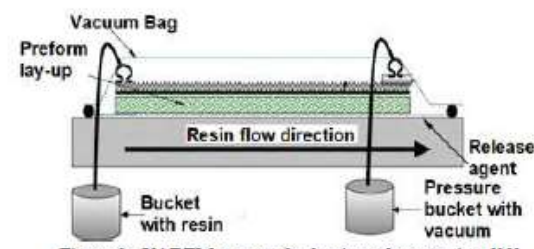


Figure 3 - VARTM process for laminated composites [32]

Anisotropy is the main feature characterising laminated composites behaviour, which means an exceptional performance along fibres direction, but deficient properties perpendicular to the fibres. Nevertheless, this sound feature is diminished by the deficient properties in the perpendicular direction to the fibres and also can be enormously affected by a failure mode which is called delamination that can occur frequently and be caused mainly by interlaminar tensile stresses [33].

Configurations in beams are crucial factors to avoid delamination; as a consequence, there were initially beams with a curved form divided into two different geometries, elliptical and semi-circular. The latter has two subtypes, unscarfed, which reported 36.85 MPa of interlaminar tensile stress (ITS) under static load is only 63% of the in-plane transverse stress. While scarfed semi-circular specimens necked down at the test section had only 32.49 MPa of ITS, which only represents 55% of in-plane transverse stress. Finally, the elliptical samples had 107.06 MPa of ITS being 194% of the in-plane transverse stress. Moisture in the samples has a positive effect because it broadens the strength distribution; the mean ITS increased up to 107.9 MPa.

On the other hand, fatigue affects strength properties negatively, reducing the mean ITS to the middle at 10^6 cycles with no stable crack propagation[33]. When the failure occurs in flat and cylindrical composites beams, cracking in intraply matrix triggers delamination and begin the damage. Delamination can be stable and progressive if intraply bending cracks create this one; however, it can be the opposite if shear cracks induce it. Moreover, response and damage extension in composites are firmly related to ply orientation[34].

Hybrid composite beams are rare in industry application. Therefore, the studies focus on the improvements contributed by the FRP materials. As for wood, it can be bonded to FRP laminates, giving the raw material beam an increment when is two layered of up to 51% and 37% for CFRP and GFRP respectively, in flexural strength [35]. As reinforcements, non-uniformly graphene platelets (GPLs) were distributed in a polymer matrix which demonstrate a most effective way to reduce bending deflections, in addition, beams with a higher weight fraction of these reinforcements distributed symmetrically are less sensitive to the nonlinear deformation[36]. Furthermore, the closer GPLs to the surface are the higher critical buckling load will suffer; this latter because GPL content affects positively also the postbuckling load-carrying [37]. Apart from the reinforcements, lamination scheme plays a vital role affecting critical buckling temperature, and thermal postbuckling path of the beam, where it can be concluded that stacking with excellent performance was $[0^\circ]_{10}$ which has the highest critical buckling temperature. Moreover, the shear stiffness increment of the elastic foundation reduces the thermally induced postbuckling deflection of the beam

[38]. On the other hand, reinforcements not only modify buckling phenomenon, but they also lead to a considerable improvement in beams, which is the case of a small portion of nanotubes [39].

Concerning optimisation through mathematical processes [40], Kalantari et al [41] stated that exist matrix voids, fibre misalignment and thickness variation as primary obstacles to reaching a successful optimisation, similarly, Mejlej et al. [42] mentioned others such as fibre failure, matrix cracking and delamination initiation. Although almost every experimental research is made scaled-down, investigations pursue an aim which is applying to large-scale demanding time and economic resources, Asl et al. mentioned that scaled-down specimens behave similarly than those made in functional scale, focusing in remaining the aspect ratio[38–40].

At the same level of importance of optimisation, behaviour prediction under low-velocity impact can be found because of the internal damages induced by low-velocity impact, in consequence, Li et al. analysed its behaviour through an extended method where remarks that the delamination size, location on the maximum displacements and the matrix crack length influence on the performance beams [46].

3. Beam composites with through-thickness reinforcements

Composites beams suffer from the same disadvantages as composites, mainly, deficiency in out-of-plane mechanical properties. This latter justifies the insertion of interlaminar reinforcements. Beams subjected to short beam shear testing with different material architecture showed there was a degradation in inter-laminar shear strength in those made of 3D woven compared to baseline plain woven composite. In contrast, there is an inversely proportional relationship between the fibres volume of z-yams and the inter-laminar shear strength. In contrast, it can say 3D woven has more damage tolerance than 2D plain woven due to the distribution of damage in the post-elastic regime. Baseline materials have excellent properties in resistance to initial damage, but consecutively, this value decreases drastically as the energy increases[47].

When stitching as reinforcement is used in beams, stitch density profoundly influences the maximum load that a beam can support, modifying this property up to a 50% extra. Also, stitching and impact force does not correlate with beginning the delamination growth; however, after initiation, stitching parameters are essential for the extent of the delamination growth. This reinforcement is sufficient for high impact energy and delamination growth, and also when the delamination occurs in the middle of the thickness[48]. In concordance with Al-Khudairi [49] *et al.* and

Ghasemnejad [50] study, stitched beams have a higher energy absorption capability and maintain the structural integrity for longer in composite wind turbine structure. Yarns volume is crucial in energy absorption because it allows the composite to support more energy impact but also increase displacement. In contrast with studies in [39–42], Ghasemnejad *et al.* [50] observed overlap region of joints stitched with Flax yarns increase the strength and impact energy absorption for nearly 70%.

Respect to interlaminar fracture toughness, Kim *et al.* [55] shows that this property as opposed to the propagation and initiation energies which come from an impact, yet Ghasemnejad [50] contradicts the latter statement, showing among their results that interlaminar fracture toughness which was enhanced by flax stitching attracts the interlaminar crack propagation satisfactorily at the interface. Another phenomenon which affects laminated beams is the buckling, and its sensitiveness depends significantly on the slenderness ratios (delamination length-span length)[56]. Numerical approaches can also determine aspects for deformation, where it can be concluded that normal deformation effect depends on span-height ratio, boundary condition and lay-ups, in addition, for thick beams, clamped-clamped boundary conditions and unsymmetrical lay-up are more significant than others [57]. Similarly, Nguyen *et al.* work shows that the optimal solutions are linked to geometric parameters such as beam length, flanges width and web's height [58].

As another crucial characteristic of beams, stiffness varies in function of the flange height, increasing its value when T-beam flange height grows. Although this height has a positive effect on energy absorption which occurs due to bending of the beam, fibre breakage and matrix crack trigger, this feature is also related to the higher flexural stiffness and strength [59].

4. Beams and joints

4.1. I-beams

I and T shape classify as variations of the cross-sectional forms of beams. Composites can be utilized as the primary material for I-beams but also as a reinforcement of a metal I-beam as Lacki *et al.* stated [46, 47], where composites enhanced twice the buckling resistance and load-bearing capacity of an aluminium alloy I-beam when a mix of polyurethane foam and glass fibre in the flanges-web zone reinforced the structure. Although when it was combined with a CFRP on the flanges, the buckling resistance and load-bearing capacity increased four times respect to the plane aluminium I-beam[60].

When a composites beam is subjected to an environment with water, similarly with operational conditions of turbine

blades, its interlaminar shear performance is reduced significantly. The reason is the cracks produced by fatigue cycling load in dry specimen were found on the inter-ply area while cracks in the immersed samples triggered the failure in the intraply area because of fibre/matrix debonding before the test[62].

An alternative method for pultruded I-beams consists in bonding web and flanges laminated with the resin being three different plates before realising and can be reinforced through a curb along the full length[63]. Feo *et al.* [49, 50] studied the axial differences respect to a pultruded beams where mentioned axial stiffness were reduced dramatically from around 10 kN/mm to the middle in bonded beams (BB) and a quarter in reinforced bonded beam (RBB) when the specimen is subjected to an end-point load. However, when the load is placed in the middle the stiffness of pultruded beams, 11.32 kN/mm, is reduced to 80% for BB and the middle for RBB. In the other hand, these relationships are not present in the beam deformation because while BB is more brittle than the plane one and RBB presents a more ductile behaviour.

A combination of glass and carbon fibres restricted to flanges make a hybrid I-beam increasing structural performance, but only using glass fibres in the web minimising costs. Flange-web length ratio affects considerably to how failure occurs. In a rate of 0.43, beams behaviour was stable and linear under bending moment, while in the 1.13 ratio, the response was the opposite in the buckling and post-buckling region; however, both behaviour configurations triggered failure delamination of the compressive flange [65]. Nevertheless, linear behaviour up to initial point failure in flexural, compression and tensile tests can be obtained by braiding, which also determines a performance without suffering delamination [66].

Other phenomena such as buckling and deflection which affect negatively I-beam are closely related to the increase in width and depth of unsupported flanges and web, as regards, the deflection is at its minimum value and critical buckling load at maximum value when the stacking sequences corresponds to (0°)_{2s} [67].

Beams are affected significantly by the environment which they are exposed to, hence, Gagani *et al.* experimented with I-beams submerged into a fluid, contributing to a high rate of saturation in composites and concluding that fibre/matrix interface is a crucial aspect in the interlaminar shear fatigue performance and its immersed fatigue behaviour improved according to the resistance of the interface [53, 59].

4.2. T-beams

T-beams are also used as lightweight structures. A configuration to improve mechanical properties is manufacturing them through three-dimensional five-

directional braided composites method at which there was a close correspondence between load-displacement curves (damage evolution) and stiffness degradation, showing a dependence of stiffness degradation with the stress level and the number of load cycles, decreasing the fatigue life with the incremental stress applied. Three stages of failure occurred in different parts, matrix cracks and resin-yarns interface debonding on the flange and fibre breaking in the web during the fatigue loading. Fibre breaking is the determinant factor for damage under the high-stress level; in contrast, the other two stages were prominent at low-stress level [69].

In some occasions, T-beams are subjected to high temperatures, where transverse impact behaviour becomes essential. Two factors influenced this behaviour, elevated temperature change failure mechanism from brittle to ductile while the temperature is increasing and transverse impact velocity being the most significant factor for transverse impact responses of the beam, which are impact peak load and total energy absorption[70]. While in a Biaxial Spacer Weft-Knitted Composite T-Beam, the impact loading is the most significant factor for the transverse impact responses[71]. Three failure mechanisms appeared in a 3D braided composites T-beam under transverse impact, matrix crack and fragmentation in the front surface and fibre breakage in the rear surface in the flange and the web position[70]. However, in a 3D orthogonal woven composite T-beam under same conditions, matrix crack occurred at the front surface, and in the meanwhile fibre breakage and matrix spallation appeared in the rear surface[72].

Yan et al. [73] compared the same reinforcement, 3D braiding, in T-beams and rectangular beams, noticing differences respect to the load-carrying capacity, where T-beams reported almost 20% of improvement respect to square ones. The increment of the number of cycles to failure under stress level of 80% was 789.6%, while for 50% was 132%; thus, flexural rigidity is enhanced by the web reducing the tension loading region area of the lower surface in a fatigue test.

When it comes to the evaluation of web's height, the height as a parameter becomes crucial to energy absorption if compared to displacement, in other words, a height of 12 mm in the web contributes a growth in 15 J, which is a increment of 300%, of energy absorption when the displacement is 9 mm [74].

4.3. T-joints

T-joints are other cross-sectional composite structures which demand a significant interest of aircraft and wind energy industries. In many cases, their performance is closely related to bonding methods, surface preparation, adherend and geometrical properties [75]–[84], such

parameters are important in the design and application of T-joints which have adhesion and bonding among their main feature[85]. However, these structures can be reinforced with through-thickness reinforcements such as z-pinning[69], [70], [71–78], [79–85], stitching [76], [79–83], [86], [87] and tufting[91], [100].

Tan et al. [94] found that Z-pinning technique does not modify the initial failure load due to the fillet region is not covered; thus this reinforcement only increased the ultimate strength in 18.3% respect to an adhered joint. This feature and traction capacity can be supported because bridging traction formation triggered the crack. Thick skin affects positively showing a higher failure initiation strength in a limited deformation while thin skin may make bridging traction surpass the bending property of the skin. Z-pinning is also a sound reinforcement for out-of-plane tensile stress, increasing 13.6% the tensile strength for the adhesive connection mode and 0.83% about stitching method, and it complements with its high capacity to deform, being at least 20% more than the usual technique of adhesion [99]. However, within the in-plane directions, interlaminar reinforcements degrade the properties. 1-thread stitching process which was proposed to minimise the main disadvantage of carbon threads, which is bending and thus preventing failure showed a reduction of around 17%, respect to unstitched specimens, but sharing values with z-pinning[98]. As a reinforced composite, it enhanced the pull-off failure strength in a range from 40.56% to 47.47% higher than the unreinforced ones, and even better than those with z-pinning reinforcement[98].

Damage detection in T-joints is indispensable to prevent crack propagation and avoid a total collapse in the structure. Li et al. [105], [106] proposed a mechanism to detect delamination in composite T-joints of wind turbines through the use of microwaves with an open-ended waveguide distinguishing the variation of flange thickness, the presence of the web incrusted into the flange and manufacturing defects. Detection could be focused primarily on the deltoid from the middle of the specimen where Xu et al. [107] noticed it is the more critical point for the beginning of Mode I debonding, on the other hand, the region with the highest stresses during mechanical pull-off load tests is at the free edges[103]. After detection, it is necessary to proceed with the repair, Cullinan et al. [108] tested to repair in situ with the use of embedded microvascular networks which create a way for the repair agent infiltration. Another method consists in creating a 3D healing network using stitching with mendable poly (ethylene-co-methacrylic acid) (EMAA) thermoplastic filament, and proceed with thermal activation which triggers repairs of delamination and matrix cracks[95].

The out-of-plane mechanical properties are frequently insufficient for many applications. In response of that, Heimbs et al. [109] made tests with metallic arrow-pin

reinforcement in a T-joint with multiples variations, where metal pins of maximum density and thermoplastic binder give an improvement in energy absorption of 720% respect to unreinforced T-joint in T-pull tests.

Sandwich composite T-joints are also widely used in different fields, with reinforcements between their concems. One of the reinforcements used was z-pinning where its efficacy is closely related to the volume content of pins where a 2% of volume content improved by around 20% and 50% the fracture strength and fracture energy respectively.

5. Implications and conclusions

Researches concerning to composites beams have been extensively developed along the past years publishing multiple scientific works. The purpose of this review comes from the necessity of observing the experimental progress of the cross-sectional form and rectangular beams and joints as an essential part of several applications. These beams working as light-weight structure had the same drawback as their primary material, existing several reinforcing techniques (e.g. stitching, z-pinning, tufting) that allow improving the out-of-plane properties. Also, composites do not only work as the primary manufacturing material but also work as reinforcements where beams are made of another material such as steel, aluminium or concrete.

There is no a considerable difference between stitching and z-pinning respect to the contribution to the out-of-plane properties, however, in the in-plane properties degradation, the difference was slightly significant, due to the harm that the yarns make on the woven. The latter was the reason for proposing variations in the stitching method such as working with only one thread. While these reinforcement processes do not include the fillet region, initial failure load will remain constant.

Notwithstanding currently the out-plane mechanical properties of the cross-sectional beams and joints are improved through different techniques, there are also others frequently used in composites that could be beneficial for these reinforcing procedures. These alternatives could be whiskers, carbon nanotubes and nonwoven fabrics. This latter could even reduce the cost of reinforcing stage due to the high volume and velocity of production. Another field of research for the future is doing extensive studies about the behaviours of the deltoid region located at the fusion region between web and flange.

POSTER PUBLISHED



Diseño de perfiles estructurales con refuerzos interlaminares en materiales compuestos

Autores: Ramírez-Elías, V; Hortúa-Díaz, O
 División de Ingenierías, Universidad de Guanajuato



Abstract

El rápido incremento en el uso industrial de estructuras ultraligeras, demanda la necesidad de hacer a los materiales compuestos interactuar con otros refuerzos interlaminares para mejorar sus propiedades mecánicas. Este trabajo se enfoca en la caracterización de perfiles I y T de vigas estandarizados de materiales compuestos con inserción de velos y su validación en un paquete (MEF).

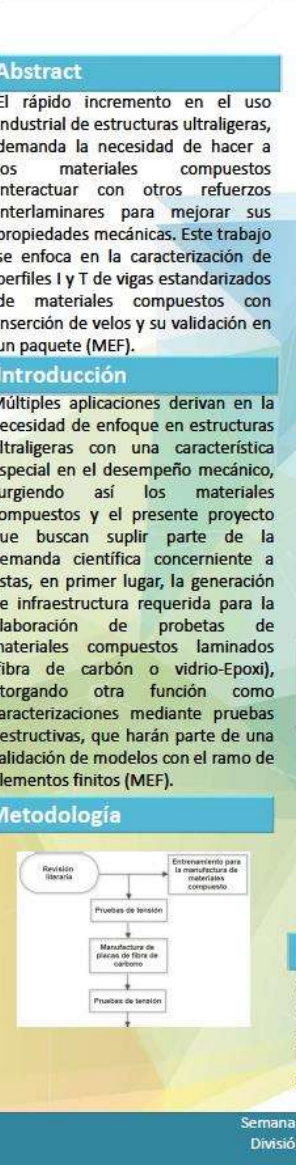
Introducción

Múltiples aplicaciones derivan en la necesidad de enfoque en estructuras ultraligeras con una característica especial en el desempeño mecánico, surgiendo así los materiales compuestos y el presente proyecto que buscan suprir parte de la demanda científica concerniente a éstas, en primer lugar, la generación de infraestructura requerida para la elaboración de probetas de materiales compuestos laminados (fibra de carbón o vidrio-Epoxi), otorgando otra función como caracterizaciones mediante pruebas destructivas, que harán parte de una validación de modelos con el ramo de elementos finitos (MEF).

Metodología

```

    graph TD
        A[Revisión literaria] --> B[Entrenamiento para la fabricación de materiales compuestos]
        B --> C[Pruebas de tensión]
        C --> D[Manufactura de placas de carbono]
        D --> E[Pruebas de tensión]
    
```



Para obtener como probeta finales, perfiles I y T con velos con refuerzos interlaminares y barrenos para aminorar su peso:

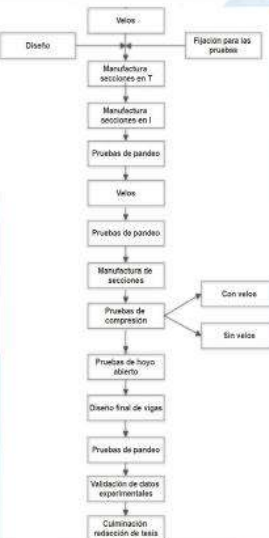


Y caracterizarlos mediante pruebas destructivas de pandeo:



Resultados y discusión

Como parte del proceso de desarrollo que se realizará se obtuvieron resultados de diseño concernientes a la sección de la realización de pruebas de pandeo.



La cual se realiza mediante un prueba con tres puntos de contacto sin existir una normativa para vigas de perfiles y T. En lo anterior se involucra un dispositivo para la fijación y otro para el aplicador de fuerza, que se necesitará fuera versátil para ambas secciones, con una versión inicial:



Y una segunda versión con mayor simplicidad en el diseño y posterior construcción:



Conclusiones

Este trabajo presenta hasta el momento un avance en lo referente a la realización de las pruebas, existiendo dificultad en el diseño debido a las pequeñas dimensiones manejadas en las probeta y la búsqueda en la simplicidad en la manufactura. Referente a las investigaciones anteriores, no se ha experimentado estos perfiles con velos como refuerzos interlaminares.

Referencias

- [1] Ramirez, V. A., Hogg, P. J., & Sampson, W. W. (2015). The influence of the nonwoven veil architectures on interlaminar fracture toughness of interleaved composites. Composites Science and Technology, 110, 103-110.
- [2] Amirhossein Hajdai, "Extending the fatigue life of a T-joint in a composite wind turbine blade," University of Manchester, 2013.
- [3] ASTM International, "D 7264 Standard Test Method for Flexural Properties of Polymer Matrix Composite Materials," ASTM Standards, vol. i. pp. 1-11, 2007.

Semana de Ingeniería Mecánica "Dr. Ricardo Chicurel Uziel"
 División de Ingenierías del Campus Irapuato – Salamanca
 25 al 29 de Marzo de 2019

70

BIBLIOGRAPHY

- [1] K.-T. Hsiao and D. Heider, *Vacuum assisted resin transfer molding (VARTM) in polymer matrix composites*. Woodhead Publishing Limited, 2012.
- [2] "VARTM cuts costs," *Reinf. Plast.*, vol. 45, no. 5, p. 22, 2001.
- [3] E. Fitzer, "The future of carbon-carbon composites," *Carbon N. Y.*, vol. 25, no. 2, pp. 163–190, 1987.
- [4] D. L. P. Andure M.W., Jirapure S.C., "Advance Automobile Material for Light Weight Future – A Review," *Int. Conf. Benchmarks Eng. Sci. Technol. ICBEST 2012*, pp. 15–22, 2012.
- [5] J. G. Hemrick, E. Lara-Curzio, E. R. Loveland, K. W. Sharp, and R. Schartow, "Woven graphite fiber structures for use in ultra-light weight heat exchangers," *Carbon N. Y.*, vol. 49, no. 14, pp. 4820–4829, 2011.
- [6] R. Sullivan, M. Rais-Rohani, T. Lacy, and N. Alday, "Structural Testing of an Ultralight UAV Composite Wing," no. May, 2012.
- [7] "AVS-SYS introduce ultra-lightweight aerospace parts," *Reinf. Plast.*, vol. 60, no. 5, p. 248, Sep. 2016.
- [8] E. P. Kasl and D. A. Crowe, "A critical review of ultralightweight composite mirror technology," *Adv. Mater. Opt. Precis. Struct. A Crit. Rev.*, vol. 10289, no. April, p. 102890B, 2017.
- [9] R. Wagner, M. Deyerler, and G. Helwig, "Advanced materials for ultralightweight stable structures," *Des. Eng. Opt. Syst. II*, vol. 3737, no. August 1999, p. 232, 2003.
- [10] H. F. A. M. J. Marzuki, "Laminate Design of Lightweight Glass Fiber Reinforced Epoxy Composite for Electrical Transmission Structure," *Procedia Chem.*, vol. 19, pp. 871–878, Jan. 2016.
- [11] T. M. Letcher, *6.13 Wind Power Fundamentals*. 2001.

- [12] J. Njuguna, *Lightweight Composite Structures in Transport*. 2016.
- [13] T. M. Letcher, *Why Wind Energy?* Elsevier Inc., 2017.
- [14] G. Marsh, "Greater role for composites in wind energy," *Reinf. Plast.*, vol. 58, no. 1, pp. 20–24, Jan. 2014.
- [15] J. Ribrant and L. M. Bertling, "Survey of failures in wind power systems with focus on Swedish wind power plants during 1997-2005," *IEEE Trans. Energy Convers.*, vol. 22, no. 1, pp. 167–173, 2007.
- [16] B. Hahn, M. Durstewitz, and K. Rohrig, "Experiences of 15 years with 1 , 500 WTs," *Components*.
- [17] S. Sheng and R. O'Connor, "Reliability of Wind Turbines," *Wind Energy Eng.*, pp. 299–327, Jan. 2017.
- [18] Tavner Peter, *Offshore Wind Turbines: Reliability, availability and maintenance*. 2013.
- [19] J. Yang *et al.*, "Structural investigation of composite wind turbine blade considering structural collapse in full-scale static tests," *Compos. Struct.*, vol. 97, pp. 15–29, Mar. 2013.
- [20] S. Huda, N. Reddy, and Y. Yang, "Ultra-light-weight composites from bamboo strips and polypropylene web with exceptional flexural properties," *Compos. Part B Eng.*, vol. 43, no. 3, pp. 1658–1664, 2012.
- [21] W. Song, X. Guan, L. Fan, W. Cao, and C. Wang, "Tuning three-dimensional textures with graphene aerogels for ultra-light flexible composites of effective electromagnetic shielding * Corresponding Authors : Tel / Fax : + 86 10 6233-3548 , email : fanlizhen@ustb.edu.cn (Li-Zhen Fan , the corresponding," *Carbon N. Y.*, vol. 3, pp. 1–10, 2015.
- [22] F. Norton S. Beckerman, Arlington, Va.; Tom Endres, Seattle, Wash.; Peter Bowthorpe, Jacksonville, "HIGH STRENGTH, LIGHT WEIGHT STRUCTURAL COMPOSITE AND METHOD OF PREPARING SAME," 1992.

- [23] A. P. Mouritz, "Compression properties of z-pinned sandwich composites," *J. Mater. Sci.*, vol. 41, no. 17, pp. 5771–5774, 2006.
- [24] M. Richard W. Lusignea, Brighton, Mass.; Joseph J. Stanco, Clinton, N.Y.; Uday Kashalikar, Natick, "FILM-BASED COMPOSITE STRUCTURES FOR ULTRALIGHTWEIGHTSD SYSTEMS," 1993.
- [25] J. S. Liu and T. J. Lu, "Multi-objective and multi-loading optimization of ultralightweight truss materials," *Int. J. Solids Struct.*, vol. 41, no. 3–4, pp. 619–635, 2004.
- [26] F. Nunes, J. R. Correia, and N. Silvestre, "Structural behavior of hybrid FRP pultruded beams: Experimental, numerical and analytical studies," *Thin-Walled Struct.*, vol. 106, pp. 201–217, 2016.
- [27] F. Nunes, N. Silvestre, and J. R. Correia, "Structural behaviour of hybrid FRP pultruded columns. Part 1: Experimental study," *Compos. Struct.*, vol. 139, pp. 291–303, 2016.
- [28] F. Nunes, N. Silvestre, and J. R. Correia, "Structural behaviour of hybrid FRP pultruded columns. Part 2: Numerical study," *Compos. Struct.*, vol. 139, pp. 304–319, 2016.
- [29] J. R. Correia, F. A. Branco, N. M. F. Silva, D. Camotim, and N. Silvestre, "First-order, buckling and post-buckling behaviour of GFRP pultruded beams. Part 1: Experimental study," *Comput. Struct.*, vol. 89, no. 21–22, pp. 2052–2064, 2011.
- [30] T. T. Nguyen, T. M. Chan, and J. T. Mottram, "Lateral-torsional buckling resistance by testing for pultruded FRP beams under different loading and displacement boundary conditions," *Compos. Part B Eng.*, vol. 60, pp. 306–318, 2014.
- [31] J. R. Correia, Y. Bai, and T. Keller, "A review of the fire behaviour of pultruded GFRP structural profiles for civil engineering applications," *Compos. Struct.*, vol. 127, pp. 267–287, 2015.

- [32] Amirhossein Hajdae, "Extending the fatigue life of a T-joint in a composite wind turbine blade," University of Manchester, 2013.
- [33] G. G. Kuka *et al.*, "Automatically produced FRP beams with embedded FOS in complex geometry: process, material compatibility, micromechanical analysis, and performance tests," *Smart Sens. Phenomena, Technol. Networks, Syst. Integr.* 2012, vol. 8346, no. February, p. 83460B, 2012.
- [34] D. Bender, J. Schuster, and D. Heider, "Flow rate control during vacuum-assisted resin transfer molding (VARTM) processing," *Compos. Sci. Technol.*, vol. 66, no. 13, pp. 2265–2271, Oct. 2006.
- [35] C. C. Hiel, M. Sumich, and D. P. Chappell, "A Curved Beam Test Specimen for Determining the Interlaminar Tensile Strength of a Laminated Composite," *J. Compos. Mater.*, vol. 25, no. 7, pp. 854–868, 1991.
- [36] L. Sheng, Z. Kutlu, and fu K. Chang, "Matrix Cracking and Delamination in Laminated Composite Beams Subjected to a Transverse Concentrated Line Load," *J. Compos. Mater.*, vol. 27, no. 5, pp. 436–470, 1993.
- [37] Y. Nadir, P. Nagarajan, M. Ameen, and M. Arif M, "Flexural stiffness and strength enhancement of horizontally glued laminated wood beams with GFRP and CFRP composite sheets," *Constr. Build. Mater.*, vol. 112, pp. 547–555, Jun. 2016.
- [38] C. Feng, S. Kitipornchai, and J. Yang, "Nonlinear bending of polymer nanocomposite beams reinforced with non-uniformly distributed graphene platelets (GPLs)," *Compos. Part B Eng.*, vol. 110, pp. 132–140, Feb. 2017.
- [39] J. Yang, H. Wu, and S. Kitipornchai, "Buckling and postbuckling of functionally graded multilayer graphene platelet-reinforced composite beams," *Compos. Struct.*, vol. 161, pp. 111–118, Feb. 2017.
- [40] Y. Kiani and M. Mirzaei, "Enhancement of non-linear thermal stability of temperature dependent laminated beams with graphene reinforcements," *Compos. Struct.*, vol. 186, pp. 114–122, Feb. 2018.

- [41] K. M. Liew, Z. X. Lei, and L. W. Zhang, "Mechanical analysis of functionally graded carbon nanotube reinforced composites: A review," *Compos. Struct.*, vol. 120, pp. 90–97, Feb. 2015.
- [42] S. Nikbakt, S. Kamarian, and M. Shakeri, "A review on optimization of composite structures Part I: Laminated composites," *Compos. Struct.*, vol. 195, pp. 158–185, Jul. 2018.
- [43] M. Kalantari, C. Dong, and I. J. Davies, "Effect of matrix voids, fibre misalignment and thickness variation on multi-objective robust optimization of carbon/glass fibre-reinforced hybrid composites under flexural loading," *Compos. Part B Eng.*, vol. 123, pp. 136–147, Aug. 2017.
- [44] V. G. Mejlej, P. Falkenberg, E. Türck, and T. Vietor, "Optimization of Variable Stiffness Composites in Automated Fiber Placement Process using Evolutionary Algorithms," *Procedia CIRP*, vol. 66, pp. 79–84, Jan. 2017.
- [45] M. E. Asl, C. Niezrecki, J. Sherwood, and P. Avitabile, "Scaled Composite I-Beams for Subcomponent Testing of Wind Turbine Blades: An Experimental Study BT - Mechanics of Composite and Multi-functional Materials, Volume 6," 2018, pp. 71–78.
- [46] M. E. Asl, C. Niezrecki, J. Sherwood, and P. Avitabile, "Experimental and theoretical similitude analysis for flexural bending of scaled-down laminated I-beams," *Compos. Struct.*, vol. 176, pp. 812–822, Sep. 2017.
- [47] M. E. Asl, C. Niezrecki, J. Sherwood, and P. Avitabile, "Similitude Analysis of Composite I-Beams with Application to Subcomponent Testing of Wind Turbine Blades BT - Experimental and Applied Mechanics, Volume 4," 2016, pp. 115–126.
- [48] M. Eydani Asl, C. Niezrecki, J. Sherwood, and P. Avitabile, "Similitude analysis of thin-walled composite I-beams for subcomponent testing of wind turbine blades," *Wind Eng.*, vol. 41, no. 5, pp. 297–312, 2017.
- [49] D. H. Li, Y. Liu, and X. Zhang, "An extended Layerwise method for composite

- laminated beams with multiple delaminations and matrix cracks," *Int. J. Numer. Methods Eng.*, vol. 101, no. 6, pp. 407–434, Oct. 2015.
- [50] T. R. Walter, G. Subhash, B. V. Sankar, and C. F. Yen, "Monotonic and cyclic short beam shear response of 3D woven composites," *Compos. Sci. Technol.*, vol. 70, no. 15, pp. 2190–2197, 2010.
- [51] B. V. Sankar and H. Zhu, "The effect of stitching on the low-velocity impact response of delaminated composite beams," *Compos. Sci. Technol.*, vol. 60, no. 14, pp. 2681–2691, 2000.
- [52] O. Al-Khudairi and H. Ghasemnejad, "To improve failure resistance in joint design of composite wind turbine blade materials," *Renew. Energy*, vol. 81, pp. 936–951, 2015.
- [53] H. Ghasemnejad, Y. Argentiero, T. A. Tez, and P. E. Barrington, "Impact damage response of natural stitched single lap-joint in composite structures," *Mater. Des.*, vol. 51, pp. 552–560, 2013.
- [54] J.-K. Kim and M.-L. Sham, "Impact and delamination failure of woven-fabric composites," *Compos. Sci. Technol.*, vol. 60, no. 5, pp. 745–761, Apr. 2000.
- [55] D. Shu, "Buckling of multiple delaminated beams," *Int. J. Solids Struct.*, vol. 35, no. 13, pp. 1451–1465, 1998.
- [56] T. P. Vo, H.-T. Thai, T.-K. Nguyen, D. Lanc, and A. Karamanli, "Flexural analysis of laminated composite and sandwich beams using a four-unknown shear and normal deformation theory," *Compos. Struct.*, vol. 176, pp. 388–397, Sep. 2017.
- [57] H. Nguyen, J. Lee, T. Vo, and D. Lanc, *Vibration and Lateral Buckling Optimisation of Thin-walled Laminated Composite Channel-section Beams*, vol. 143. 2016.
- [58] Jiwei Zhang, Hong Hu, Baozhong Sun, and Bohong Gu, "Dynamic Responses of 3-D Multi-structured Knitted Composite T-beam under Transverse Impact," *J. Compos. Mater.*, vol. 44, no. 2, pp. 157–180, 2009.

- [59] P. Lacki, A. Derlatka, and J. Winowiecka, "Analysis of the composite I-beam reinforced with PU foam with the addition of chopped glass fiber," *Compos. Struct.*, vol. 218, pp. 60–70, Jun. 2019.
- [60] A. I. Gagani, E. P. V. Mialon, and A. T. Echtermeyer, "Immersed interlaminar fatigue of glass fiber epoxy composites using the I-beam method," *Int. J. Fatigue*, vol. 119, pp. 302–310, Feb. 2019.
- [61] F. Ascione, L. Feo, M. Lamberti, and R. Penna, "Experimental and numerical evaluation of the axial stiffness of the web-to-flange adhesive connections in composite I-beams," *Compos. Struct.*, vol. 176, pp. 702–714, Sep. 2017.
- [62] L. Feo, A. S. Mosallam, and R. Penna, "Mechanical behavior of web–flange junctions of thin-walled pultruded I-profiles: An experimental and numerical evaluation," *Compos. Part B Eng.*, vol. 48, pp. 18–39, May 2013.
- [63] A. Fascetti, L. Feo, N. Nisticò, and R. Penna, "Web-flange behavior of pultruded GFRP I-beams: A lattice model for the interpretation of experimental results," *Compos. Part B Eng.*, vol. 100, pp. 257–269, Sep. 2016.
- [64] N. D. Hai, H. Mutuyoshi, S. Asamoto, and T. Matsui, "Structural behavior of hybrid FRP composite I-beam," *Constr. Build. Mater.*, vol. 24, no. 6, pp. 956–969, 2010.
- [65] S. S. Yau, T. W. Chou, and F. K. Ko, "Flexural and axial compressive failures of three-dimensionally braided composite I-beams," *Composites*, vol. 17, no. 3, pp. 227–232, 1986.
- [66] S. Singh, H. Chawla, and P. Munjal, *Effect of Shear Deformation on Flexural Response of Laminated Composite I-Beam*. 2015.
- [67] A. I. Gagani, A. B. Monsås, A. E. Krauklis, and A. T. Echtermeyer, "The effect of temperature and water immersion on the interlaminar shear fatigue of glass fiber epoxy composites using the I-beam method," *Compos. Sci. Technol.*, vol. 181, p. 107703, Sep. 2019.
- [68] Y. Ouyang, H. Wang, B. Gu, and B. Sun, "Experimental study on the bending

- fatigue behaviors of 3D five directional braided T-shaped composites," *J. Text. Inst.*, vol. 109, no. 5, pp. 603–613, 2018.
- [69] W. Zhang, B. Gu, and B. Sun, "Transverse impact behaviors of 3D braided composites T-beam at elevated temperatures," *J. Compos. Mater.*, vol. 50, no. 28, pp. 3961–3971, 2016.
- [70] M. Zhang, B. Sun, H. Hu, and B. Gu, "Dynamic behavior of 3D biaxial spacer weft-knitted composite T-beam under transverse impact," *Mech. Adv. Mater. Struct.*, vol. 16, no. 5, pp. 356–370, 2009.
- [71] A. Hao, B. Sun, Y. Qiu, and B. Gu, "Dynamic properties of 3-D orthogonal woven composite T-beam under transverse impact," *Compos. Part A Appl. Sci. Manuf.*, vol. 39, no. 7, pp. 1073–1082, 2008.
- [72] J. Yan, K. Liu, H. Zhou, Z. Zhang, B. Gu, and B. Sun, "The bending fatigue comparison between 3D braided rectangular composites and T-beam composites," *Fibers Polym.*, vol. 16, no. 3, pp. 634–639, 2015.
- [73] L. LV, X. ZHANG, S. YAN, Y. QIAN, and F. YE, "Bending Properties of T-Shaped 3-D Integrated Woven Composites: Experiment and FEM Simulation," *J. Fiber Sci. Technol.*, vol. 73, no. 7, pp. 170–176, 2017.
- [74] L. Liao, C. Huang, and T. Sawa, "Effect of adhesive thickness, adhesive type and scarf angle on the mechanical properties of scarf adhesive joints," *Int. J. Solids Struct.*, vol. 50, no. 25–26, pp. 4333–4340, 2013.
- [75] S. Akpinar, "Effects of laminate carbon/epoxy composite patches on the strength of double-strap adhesive joints: Experimental and numerical analysis," *Mater. Des.*, vol. 51, pp. 501–512, 2013.
- [76] M. Kanerva and O. Saarela, "The peel ply surface treatment for adhesive bonding of composites: A review," *Int. J. Adhes. Adhes.*, vol. 43, pp. 60–69, 2013.
- [77] L. F. M. da Silva, R. J. C. Carbas, G. W. Critchlow, M. A. V. Figueiredo, and K. Brown, "Effect of material, geometry, surface treatment and environment on

- the shear strength of single lap joints," *Int. J. Adhes. Adhes.*, vol. 29, no. 6, pp. 621–632, 2009.
- [78] G. Meneghetti, M. Quaresimin, and M. Ricotta, "Influence of the interface ply orientation on the fatigue behaviour of bonded joints in composite materials," *Int. J. Fatigue*, vol. 32, no. 1, pp. 82–93, 2010.
- [79] M. Mokhtari, K. Madani, M. Belhouari, S. Touzain, X. Feaugas, and M. Ratwani, "Effects of composite adherend properties on stresses in double lap bonded joints," *Mater. Des.*, vol. 44, pp. 633–639, 2013.
- [80] A. Moradi, N. Carrère, D. Leguillon, E. Martin, and J. Y. Cognard, "Strength prediction of bonded assemblies using a coupled criterion under elastic assumptions: Effect of material and geometrical parameters," *Int. J. Adhes. Adhes.*, vol. 47, pp. 73–82, 2013.
- [81] T. C. Nguyen, Y. Bai, X. L. Zhao, and R. Al-Mahaidi, "Curing effects on steel/CFRP double strap joints under combined mechanical load, temperature and humidity," *Constr. Build. Mater.*, vol. 40, pp. 899–907, 2013.
- [82] S.-J. Shin *et al.*, "Effect of manufacturing methods on the shear strength of composite single-lap bonded joints," *Compos. Struct.*, vol. 92, no. 9, pp. 2194–2202, 2009.
- [83] F. Stazi, M. Giampaoli, M. Rossi, and P. Munafò, "Environmental ageing on GFRP pultruded joints: Comparison between different adhesives," *Compos. Struct.*, vol. 133, pp. 404–414, 2015.
- [84] S. Budhe, M. D. Banea, S. de Barros, and L. F. M. da Silva, "An updated review of adhesively bonded joints in composite materials," *Int. J. Adhes. Adhes.*, vol. 72, no. October 2016, pp. 30–42, 2017.
- [85] L. Burns, A. P. Mouritz, D. Pook, and S. Feih, "Strengthening of composite T-joints using novel ply design approaches," *Compos. Part B Eng.*, vol. 88, pp. 73–84, 2016.
- [86] P. B. Stickler and M. Ramulu, "Experimental study of composite T-joints under

- tensile and shear loading," *Adv. Compos. Mater. Off. J. Japan Soc. Compos. Mater.*, vol. 15, no. 2, pp. 193–210, 2006.
- [87] T. M. Koh, S. Feih, and A. P. Mouritz, "Strengthening mechanics of thin and thick composite T-joints reinforced with z-pins," *Compos. Part A Appl. Sci. Manuf.*, vol. 43, no. 8, pp. 1308–1317, 2012.
- [88] Y. Bin Park, B. H. Lee, J. H. Kweon, J. H. Choi, and I. H. Choi, "The strength of composite bonded T-joints transversely reinforced by carbon pins," *Compos. Struct.*, vol. 94, no. 2, pp. 625–634, Jan. 2012.
- [89] Y. Tan, Y. Li, D. Huan, X. Zhang, and Q. Chu, "Failure analysis and strengthening mechanism of Z-pinned composite T-joints under tensile loading," *Sci. Eng. Compos. Mater.*, vol. 24, no. 5, pp. 783–790, 2017.
- [90] Z. L. Liu, P. R. Jia, T. Peng, and Z. L. Yao, "Study on Tensile Mechanical Behavior of Composite T-Joints," *Adv. Mater. Res.*, vol. 1142, pp. 146–151, 2017.
- [91] C. H. Kim, D. H. Jo, and J. H. Choi, "Failure strength of composite T-joints prepared using a new 1-thread stitching process," *Compos. Struct.*, vol. 178, pp. 225–231, 2017.
- [92] R. Sloan, C. Soutis, A. Gibson, N. Karimian, A. Haigh, and Z. Li, "Delamination Detection in Composite T-Joints of Wind Turbine Blades using Microwaves," *Adv. Compos. Lett.*, vol. 25, no. 4, p. 096369351602500, 2016.
- [93] Z. Li, A. Haigh, R. Sloan, A. Gibson, and N. Karimian, "Microwave imaging for delamination detection in t-joints of wind turbine composite blades," *Eur. Microw. Week 2016 "Microwaves Everywhere"*, *EuMW 2016 - Conf. Proceedings; 46th Eur. Microw. Conf. EuMC 2016*, pp. 1235–1238, 2016.
- [94] X. Xu, M. R. Wisnom, S. R. Hallett, G. Holden, and B. Gordon, "Predicting Debonding and Delamination in Adhesively Bonded T-joints," in *17th European Conference on Composite Materials*, 2016, no. June, pp. 26–30.
- [95] F. Hélenon, M. R. Wisnom, S. R. Hallett, and R. S. Trask, "Numerical

- investigation into failure of laminated composite T-piece specimens under tensile loading," *Compos. Part A Appl. Sci. Manuf.*, vol. 43, no. 7, pp. 1017–1027, 2012.
- [96] J. F. Cullinan, M. R. Wisnom, and I. P. Bond, "Damage Manipulation and In Situ Repair of Composite T-Joints," *J. Aircr.*, vol. 53, no. 4, pp. 1013–1021, 2016.
- [97] T. Yang, J. Zhang, A. P. Mouritz, and C. H. Wang, "Healing of carbon fibre-epoxy composite T-joints using mendable polymer fibre stitching," *Compos. Part B Eng.*, vol. 45, no. 1, pp. 1499–1507, 2013.
- [98] S. Heimbs, M. Jurgens, C. Breu, G. Ganzenmuller, and J. Wolfrum, "Investigation and Improvement of Composite T-Joints with Metallic Arrow-Pin Reinforcement," in *Joining Technologies for Composites and Dissimilar Materials*, vol. 10, 2017.
- [99] V. A. Ramirez, P. J. Hogg, and W. W. Sampson, "The influence of the nonwoven veil architectures on interlaminar fracture toughness of interleaved composites," *Compos. Sci. Technol.*, vol. 110, pp. 103–110, 2015.
- [100] M. Kuwata and P. J. Hogg, "Interlaminar toughness of interleaved CFRP using non-woven veils: Part 1. Mode-I testing," *Compos. Part A Appl. Sci. Manuf.*, vol. 42, no. 10, pp. 1551–1559, Oct. 2011.
- [101] M. Kuwata, S. Matsuda, H. Kishi, A. Murakami, and P. Hogg, "Impact Resistance of Interleaved FRP Using Non-Woven Fabric as Interleaf Materials," *J. Japan Soc. Compos. Mater.*, vol. 33, pp. 55–61, Jan. 2007.
- [102] E. Armstrong-Carroll and R. Cochran, "Improvement of Delamination Resistance with Carbon Nonwoven Mat Interleaves," in *Composite Materials: Fatigue and Fracture: Fifth Volume*, R. H. Martin, Ed. West Conshohocken, PA: ASTM International, 1995, pp. 124–131.
- [103] Y. Aono, S. Murae, and T. Kubo, "Static Mechanical Properties of GFRP Laminates with Waste GFRP Interleaf," *Procedia Eng.*, vol. 10, pp. 2080–

- 2085, Jan. 2011.
- [104] J. A. VanderVennet *et al.*, "Fracture toughness characterization of nanoreinforced carbon-fiber composite materials for damage mitigation," in *Proc. SPIE*, 2011, vol. 7978.
 - [105] S.-H. Lee, H. Noguchi, Y.-B. Kim, and S.-K. Cheong, "Effect of Interleaved Non-Woven Carbon Tissue on Interlaminar Fracture Toughness of Laminated Composites: Part II – Mode I," *J. Compos. Mater.*, vol. 36, no. 18, pp. 2169–2181, Sep. 2002.
 - [106] S.-H. Lee, H. Noguchi, Y.-B. Kim, and S.-K. Cheong, "Effect of Interleaved NonWoven Carbon Tissue on Interlaminar Fracture Toughness of Laminated Composites: Part I – Mode II," *J. Compos. Mater. - J Compos MATER*, vol. 36, pp. 2153–2168, Sep. 2002.
 - [107] S.-H. Lee, J.-H. Lee, S.-K. Cheong, and H. Noguchi, "A toughening and strengthening technique of hybrid composites with non-woven tissue," *J. Mater. Process. Technol.*, vol. 207, no. 1, pp. 21–29, 2008.
 - [108] E. J. Barbero, *Finite element analysis of composite materials using ANSYS*. CRC press, 2013.